Accurate analytic potentials for $Li_2(X\ ^1\Sigma_g^+)$ and $Li_2(A\ ^1\Sigma_u^+)$ from 2 to 90 Å, and the radiative lifetime of Li(2*p*)

Robert J. Le Roy,[1,a)] Nikesh S. Dattani,[1] John A. Coxon,[2] Amanda J. Ross,[3] Patrick Crozet,[3] and Colan Linton[4]
[1]*Department of Chemistry, University of Waterloo, Waterloo, Ontario N2L 3G1, Canada*
[2]*Department of Chemistry, Dalhousie University, Halifax, Nova Scotia B3H 4J3, Canada*
[3]*Laboratoire de Spectrométrie Ionique et Moléculaire, UMR 5579 Université Lyon 1 and CNRS, Université de Lyon, 43 Bd. du 11 Novembre 1918, Villeurbanne Cedex 69622, France*
[4]*Department of Physics, University of New Brunswick, Fredericton, New Brunswick E3B 5A3, Canada*

(Received 7 August 2009; accepted 27 October 2009; published online 25 November 2009)

Extensions of the recently introduced "Morse/long-range" (MLR) potential function form allow a straightforward treatment of a molecular state for which the inverse-power long-range potential changes character with internuclear separation. Use of this function in a direct-potential-fit analysis of a combination of new fluorescence data for $^{7,7}Li_2$, $^{6,6}Li_2$, and $^{6,7}Li_2$ with previously reported data for the $A(^1\Sigma_u^+)$ and $X(^1\Sigma_g^+)$ states yields accurate, fully analytic potentials for both states, together with the analytic "adiabatic" Born–Oppenheimer breakdown radial correction functions which are responsible for the difference between the interaction potentials and well depths for the different isotopologues. This analysis yields accurate well depths of $\mathfrak{D}_e=8516.709(\pm0.004)$ and $8516.774(\pm0.004)$ cm^{-1} and scattering lengths of $18.11(\pm0.05)$ and $23.84(\pm0.05)$ Å for the ground-states of $^{7,7}Li_2$ and $^{6,6}Li_2$, respectively, as well as improved atomic radiative lifetimes of $\tau(2p)=27.1018(\pm0.0014)$ ns for $^7Li(2p)$ and $27.1024(\pm0.0014)$ ns for $^6Li(2p)$. © *2009 American Institute of Physics*. [doi:10.1063/1.3264688]

I. INTRODUCTION

As the lightest uncharged nonhydride diatomic molecule, Li_2 has long had a special role as a testing ground for theory and experiment. Its spectroscopy has been studied extensively, both experimentally and theoretically, and a large amount of accurate data for both $^{7,7}Li_2$ and $^{6,6}Li_2$ in many valence and Rydberg electronic states have been accumulated and classified. Work at Rice University pioneered studies of the formation of lithium dimers by photoassociation (PAS) of ultracold gases,[1] and of Bose–Einstein condensates of lithium.[2] Extracting accurate atomic lifetime data from molecular spectra via knowledge of the long-range interaction potential was shown to be more reliable than direct determination.[3,4]

Two features which distinguish Li from the heavier alkali atoms[5] are the facts that hyperfine interactions are very weak, and that the ^2P fine structure splitting is very small (0.34 cm^{-1}, or 0.48 K in terms of atomic trap depth) and happens to be comparable to the difference between the atomic D-line transition energies for ^6Li and ^7Li.[6] This fine-structure splitting is too small to produce the extensive spin-orbit perturbations characterizing the short-range interactions between the $A\ ^1\Sigma_u^+$ and $b\ ^3\Pi_u$ states of the heavier alkali dimers, for which only a full coupled-channel treatment can explain the complete set of observed energy levels. Coupled-channel analyses such as those developed by Bergeman and co-workers[7] and by Zaitsevskii and co-workers[8] have been remarkably successful in their description of (*inter alia*) the $A\ ^1\Sigma_u^+$ state of Na_2 to within 1 cm^{-1} of the $^2S+^2P_{1/2}$ asymptote, and of heavier alkali molecules such as NaRb. However, because both spin-orbit and potential energy functions need to be determined from the same set of observations, it is much harder to reproduce such data to the level of experimental uncertainty, and to highlight small but significant effects such as Born–Oppenheimer breakdown (BOB). In contrast, Li_2 is unique among the alkali dimers because (ignoring hyperfine structure) the energy levels of the singlet states correlating with the $ns+np$ asymptote can be derived from potential curves without having to take account of J-dependent spin-orbit mixing. Because lithium is such a light atom, there has also been a great deal of interest in using Li_2 to investigate BOB by looking for differences between the level energy patterns and potential energy functions of $^{7,7}Li_2$ and $^{6,6}Li_2$. This in turn led to efforts to construct accurate, isotopically distinct potential curves for various electronic states which are able to reproduce all of the available experimental data within their uncertainties.

Over the years, particular attention has been paid to the two lowest-lying singlet states of Li_2, $X\ ^1\Sigma_g^+$ and $A\ ^1\Sigma_u^+$, and there have been several attempts to construct accurate potential curves for them.[9–16] However, the commonly used approach of fitting the level energies to parametrized expressions (e.g., Dunham expansions) and then applying the first-order RKR inversion procedure[17–20] (with or without perturbative quantum mechanical "IPA" corrections[21,22]) has

a)Electronic mail: leroy@uwaterloo.ca.

a number of shortcomings. In particular, the Dunham polynomial expressions most commonly used to represent vibration-rotation level energies are notoriously unreliable for extrapolation, which makes it difficult to determine accurate values of the dissociation energy in that manner. RKR potentials also often have irregular repulsive inner walls which turn inward or outward in an unphysical manner, and the fact that the RKR method is a first-order semiclassical procedure means that quantum calculations using such potentials cannot accurately reproduce the original experimental level spacings, especially for small-reduced-mass systems. There are also problems associated with smoothly connecting the RKR turning points spanning the data region[23] both to a realistic short-range repulsive wall and to a long-range function extrapolating properly to the dissociation limit. Even when the above errors are small, they may still suffice to preclude quantitative determination of the small differences between potentials for different isotopologues (e.g., differences in $\mathfrak{D}_e$) due to BOB.

Over the past decade or so, most of the above problems have been resolved by the development of the fully quantum mechanical, numerical direct-potential-fit (DPF) method of data analysis, in which parameters defining an analytic potential energy function are determined from direct fits to spectroscopic data. This approach eliminates the need to calculate the traditional molecular spectroscopic constants, and it generally requires far fewer parameters to represent a given data set accurately. However, developing optimally flexible and robust potential function forms which naturally incorporate the correct physical long-range behavior has been a significant challenge.

Coxon and Melville recently used the DPF approach to analyze data for the $X\ ^1\Sigma_g^+$ and $A\ ^1\Sigma_u^+$ states of Li_2 by fitting simultaneously to almost all of the then-available data for the $A\ ^1\Sigma_u^+ - X\ ^1\Sigma_g^+$ and $E,F(^1\Sigma_g^+) - A(^1\Sigma_u^+)$ systems for $^{7,7}Li_2$ and $^{6,6}Li_2$, together with the one data set that was available for the $A(^1\Sigma_u^+) - X(^1\Sigma_u^+)$ system of $^{6,7}Li_2$.[24] The data used in their analysis extend up to $v=84$ of the A state of $^{6,6}Li_2$, which lies $\sim 2.4\ cm^{-1}$ below dissociation and has an outer turning point of approximately 52 Å, but only to $v(A)=62$ for $^{7,7}Li_2$, which lies some $206\ cm^{-1}$ below dissociation and has an outer turning point of only 12.1 Å, and to $v(A)=5$ for $^{6,7}Li_2$. Moreover, their analysis excluded PAS results which determined the binding energies of the rotationally cold, highly excited vibrational levels $v(A)=83$ for $^{6,7}Li_2$,[25] $v(A)=62-88$ for $^{6,6}Li_2$,[1] and $v(A)=65-97$ for $^{7,7}Li_2$,[1] the highest of which is bound by only $0.38\ cm^{-1}$ and has an outer turning point of almost 90 Å. The PAS data could not be accounted for because the long-range tail of the potential function form they used consisted of only a single (C_3/r^3) inverse-power term, and the fact that the value of this C_3 coefficient changes with the transition from Hund's case (a) to case (c) coupling at very large distances was neglected. As a result, the asymptote of their potential does not correlate with the real A-state limit of dissociation to $Li(^2S_{1/2}) + Li(^2P_{1/2})$, but rather extrapolates to a nonphysical limit some 2/3 of the distance from there to the asymptote for $Li(^2S_{1/2}) + Li(^2P_{3/2})$, which lies $\approx 0.335\ cm^{-1}$ to higher energy. In view of the above, an important challenge addressed in this work is to devise an analytic potential function which incorporates the actual long-range behavior of the A-state interaction.

One object of the present work was to extend the "conventional" experimental vibrational data sets for the $A\ ^1\Sigma_u^+$ states of $^{7,7}Li_2$ and $^{6,7}Li_2$ to fill in the gap between the existing results and the PAS data of Abraham *et al.*[1] and of Schlöder *et al.*[25] Our new perturbation-dependent experiments (described below) on $^{6,7}Li_2$ extend the range of its observed vibrational levels to $v(A)=71$ [cf. to $v(A)=5$], while our new data for $^{7,7}Li_2$ include additional vibrational levels of the A state, which now overlap the vibrational range of the PAS data for this isotopologue. However, our new data for $^{7,7}Li_2$ involved rotational levels in the range $J=14-25$, so no direct comparison with the levels $J \leq 2$ seen by PAS was possible. Thus, extraction of a reliable dissociation energy from these data relied heavily on the quality of the potential energy function used in the analysis. A second objective was therefore to address the challenge of developing a unified form for the potential energy function which would be compact and easily "portable" (requiring relatively few parameters), robust (allowing stable convergence in fits), "well behaved" (providing physically realistic extrapolation outside the "data region"), and in which key physically interesting properties such as the well depth, equilibrium distance, and long-range potential coefficients are natural parameters. This challenge led to the development of the extended "Morse/long-range" (MLR) potential function form described in Sec. III. The use of this potential form in a global multi-isotopologue analysis of data for the $X\ ^1\Sigma_g^+$ and $A\ ^1\Sigma_u^+$ states of Li_2 is then presented in Sec. IV.

II. EXPERIMENTAL

The type of experiments that allowed us to observe levels up to $v=84$ in the $A\ ^1\Sigma_u^+$ state of $^{6,6}Li_2$ was described in detail in Ref. 11. The new $^{7,7}Li_2$ data reported herein were obtained following the same approach used there: optical-optical double resonance (OODR) was used to excite the $(4)F\ ^1\Sigma_g^+$ state via $X\ ^1\Sigma_g^+ \rightarrow A\ ^1\Sigma_u^+ \rightarrow F\ ^1\Sigma_g^+$ transitions, and the resulting fluorescence was detected at high resolution with a Fourier transform spectrometer. An Ar^+ laser pumped two-ring dye laser was operated with DCM and R6G dyes, and the resulting tunable cw beams excited Li_2 which had been formed in a heat pipe at temperatures of 750–850 °C.

The work on $^{6,6}Li_2$ had shown that fluorescence from the $(4)F\ ^1\Sigma_g^+$ state occurred to vibrational levels of $A\ ^1\Sigma_u^+$ above $v(A)=30$ (i.e., levels with outer turning points beyond 6.2 Å) only when the laser selected upper-state levels of mixed $(4)F\ ^1\Sigma_g^+/(3)E\ ^1\Sigma_g^+$ character (i.e., when F and E levels with the same J were almost in resonance).[11] This excitation-plus-fluorescence mechanism, which is illustrated by Fig. 7 of Ref. 11, is based on the fact that the E state potential has a "shelf" that lies below the F state curve. The outer turning points of E-state levels lying above the shelf are relatively large and favor fluorescence into A-state levels lying relatively close to dissociation. However, poor vibrational over-

TABLE I. Observed coincidences between $F\ ^1\Sigma_g^+$ and $E\ ^1\Sigma_g^+$ levels in $^{7,7}Li_2$, with transition wavenumbers in cm^{-1}.

$v(F)$	$v(E)$	J (obs)	max$\{v_A\}$	$A-X$ resonance		$\begin{cases}F-A & \text{resonance}\\ E-A & \text{resonance}\end{cases}$	
3	26	18	46	$R(16)$ 4–0	14 973.98	$R(17)$ 3–4	15 544.92
						$R(17)$ 26–4	15 544.51
4	28	8	49	$P(10)$ 3–0	14 737.68	$P(9)$ 4–3	15 994.77
						$P(9)$ 28–3	15 993.78
7	34	25	77	$R(25)$ 2–0	14 427.46	$P(26)$ 7–2	16 778.80
						$P(26)$ 34–2	16 776.44
8	36	22, 23	83	$R(20)$ 3–0	14 708.42	$R(21)$ 8–3	16 787.63
						$R(21)$ 36–3	16 793.61
				$R(21)$ 3–0	14 701.43	$R(22)$ 8–3	16 784.66
						$R(22)$ 36–3	16 782.72
9	40	20, 21	88	$R(18)$ 3–0	14 721.27	$R(19)$ 9–3	16 985.42
						$R(19)$ 40–3	16 990.55
				$R(19)$ 3–0	14 715.04	$R(20)$ 9–3	16 982.73
						$R(20)$ 40–3	16 980.52
10	42	19, 20	88	$R(17)$ 4–0	14 965.29	$R(18)$ 10–4	16 934.73
						$R(18)$ 42–4	16 936.57
12	46	17	71	$P(19)$ 5–0	15 157.34	$P(18)$ 12–5	17 034.66
						$P(18)$ 46–5	17 036.46

lap prevents direct access to these levels via $X\ ^1\Sigma_g^+ \rightarrow A\ ^1\Sigma_u^+ \rightarrow E\ ^1\Sigma_g^+$ excitation. The OODR process favors excitation to the F state, but the internuclear separation at the outer limb of the F state potential is too small to allow transitions into levels near the top of the A-state well to be observed in this energy region. Although the F-state potential also has a shelf, starting at $v \sim 33$, vibrational levels lying above that shelf mainly predissociate into the E state continuum rather than give rise to $F \rightarrow A$ fluorescence.[26]

In the present work, "normal" fluorescence from low vibrational levels of the F-state of $^{7,7}Li_2$ consisted of strong near-infrared fluorescence into the $B\ ^1\Pi_u$ state plus much weaker visible transitions into low ($v \lesssim 20$) levels of the $A\ ^1\Sigma_u^+$ state. In contrast, fluorescence into levels near the top of the A-state well is totally dependent on chance coincidences and interactions between E- and F-state levels, which means that data could be obtained only for a very limited selection of J values. For $^{6,6}Li_2$ such perturbations occurred mostly at low J ($J \sim 5$), whereas for $^{7,7}Li_2$ the J values were generally higher: $J=14-25$. Table I lists the observed vibrational and rotational quantum numbers, v and J, of interacting E and F levels that were used in our new $^{7,7}Li_2$ experiments. Figure 1 shows one of the most extensive fluorescence series recorded, originating in $v(E)=40$, $J=21$, which yielded observable emission into A state levels $v(A)=36-88$. Although the overall vibrational intensity pattern resembles that seen for $^{6,6}Li_2$, relative intensities of the $R(J-1)$ and $P(J+1)$ lines in the higher-J spectra for $^{7,7}Li_2$ contrast sharply with those observed in the low J transitions recorded for $^{6,6}Li_2$. Since the rotational spacing between the R and P lines in the rotational doublets is more than half the vibrational interval when $v \geq 75$, the Franck–Condon factors show a strong dependence on J, and there is a very large difference in the intensities of R and P lines at a given v'', particularly for $60 \lesssim v(A) \lesssim 80$ where the potential curve flattens out and takes on asymptotic character. This was not true at the lower J values observed in $^{6,6}Li_2$ experiments for which the R and P lines were of almost equal intensity in nearly all bands.

For the mixed isotopologue $^{6,7}Li_2$ we obtained new rotationally relaxed $A \rightarrow X$ fluorescence series ($v'=19$, $v''=25$ and 26) and a long progression of $F,E \rightarrow A$ doublets [from $J'=17$, $v'(E)=39$] from our OODR experiments. These new data greatly extend the range of observed vibrational levels for this isotopologue to $v(X)=33$ and $v(A)=71$ [cf. $v_{max}(X)=3$ and $v_{max}(A)=5$ in Ref. 24].

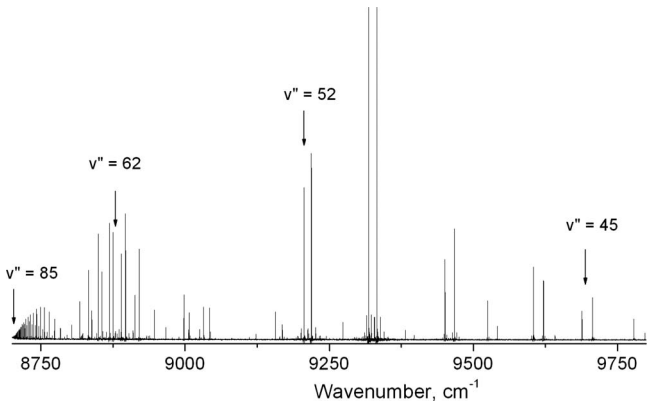

FIG. 1. Fluorescence series originating from $v=40$, $J=21$ of the $E\ ^1\Sigma_g^+$ state (mixed with $v=9$ of the F state) of $^{7,7}Li_2$.

III. THE MORSE/LONG-RANGE MODEL FOR POTENTIAL ENERGY FUNCTIONS

A. The basic MLR model

The basic MLR model for radial potential energy functions has the form[27–30]

$$V_{\mathrm{MLR}}(r) = \mathcal{D}_e\left[1 - \frac{u_{\mathrm{LR}}(r)}{u_{\mathrm{LR}}(r_e)}e^{-\beta(r)\cdot y_p(r)}\right]^2, \tag{1}$$

in which $\mathcal{D}_e$ is the well depth, $u_{\mathrm{LR}}(r)$ is a function which defines the (attractive) long-range behavior of the potential energy function to be

$$V(r) \simeq V_{\mathrm{LR}}(r) = \mathcal{D}_e - u_{\mathrm{LR}}(r), \tag{2}$$

and the denominator factor $u_{\mathrm{LR}}(r_e)$ is the value of that function at the equilibrium bond length, r_e. The radial behavior of this function is expressed in terms of the dimensionless radial variable

$$y_p(r) = y_p^{\mathrm{eq}}(r) = \frac{r^p - r_e^p}{r^p + r_e^p}, \tag{3}$$

in which p is an integer greater than 1 whose value is partly defined (i.e., given a lower bound) by the nature of the model chosen for the long-range potential $u_{\mathrm{LR}}(r)$. The exponent coefficient function $\beta(r)$ is a (fairly) slowly varying function of r, which is written as a polynomial constrained to approach a specified value (β_∞) as $r\to\infty$ [or $y_p(r)\to 1$]:

$$\beta(r) = y_p(r)\beta_\infty + [1 - y_p(r)]\sum_{i=0}^{\{N_S,N_L\}}\beta_i y_p(r)^i, \tag{4}$$

while the definition of $y_p(r)$ and the algebraic structure of Eqs. (1)–(4) means that $\lim_{r\to\infty}\beta(r)\equiv\beta_\infty=\ln\{2\mathcal{D}_e/u_{\mathrm{LR}}(r_e)\}$.

In order to prevent unphysical behavior in the short-range region (e.g., potential turnover), the upper bound on the summation in Eq. (4) had been allowed to have the different values $N=N_S$ for $r<r_e$ and N_L for $r\geq r_e$.[31] For cases in which $N_S\neq N_L$, at the one distance $r=r_e$ there would be small discontinuities in derivatives of the potential of order $\geq(\min\{N_S,N_L\}+2)$. However, in typical cases $\min\{N_S,N_L\}\geq 5$,[27–30] so this is not a significant shortcoming. In any case, the extensions of the model presented below seem to removed the need for allowing $N_L\neq N_S$.

The term $u_{\mathrm{LR}}(r)$ in Eq. (1) defines the attractive (positive terms corresponding to attraction) long-range behavior to be imposed on the potential function. In general, long-range potentials are defined by a sum of inverse-power terms

$$u_{\mathrm{LR}}(r) = \sum_{i=1}^{\mathrm{last}}\frac{C_{m_i}}{r^{m_i}} = \frac{C_{m_1}}{r^{m_1}} + \frac{C_{m_2}}{r^{m_2}} + \cdots + \frac{C_{m_{\mathrm{last}}}}{r^{m_{\mathrm{last}}}}, \tag{5}$$

in which the integer powers m_i and coefficients C_{m_i} are determined by the nature of the atoms to which the given state dissociates and the symmetry of the particular molecular electronic state.[32–36] A summary of rules governing which terms contribute to the long-range potential for a given case may be found in Refs. 36–38.

As discussed in Ref. 28, the integer power "p" defining the radial variable of Eq. (3) must be greater than the difference between the largest and smallest (inverse) powers of the terms included in the chosen definition of $u_{\mathrm{LR}}(r)$: $p>(m_{\mathrm{last}}-m_1)$. In practice, it is often desirable to set p equal to the difference between the leading power m_1 and the power of the first long-range term predicted by theory which is *not* included in the chosen definition of $u_{\mathrm{LR}}(r)$, $p=(m_{\mathrm{next}}-m_1)$, as this would mean that the leading contribution of the exponential term in Eq. (1) to the long-range potential would have the same radial behavior as that first missing term, $1/r^{m_{\mathrm{next}}}$.

B. Extensions of the MLR model

1. Addressing a problem associated with $m_1=3$ long-range potentials

If the integer p defining the radial expansion variable $y_p(r)$ is chosen so that $p>(m_{\mathrm{last}}-m_1)$, at sufficiently large r, the exponential term in Eq. (1) becomes $e^{-\beta_\infty}=u_{\mathrm{LR}}(r_e)/(2\mathcal{D}_e)$ and Eq. (1) becomes

$$V_{\mathrm{MLR}}(r) \simeq \mathcal{D}_e - u_{\mathrm{LR}}(r) + \frac{1}{4\mathcal{D}_e}[u_{\mathrm{LR}}(r)]^2. \tag{6}$$

For a species (such as ground-state Li_2) which dissociates to yield two S-state atoms, theory tells us that the leading terms contributing to the long-range potential have powers $m=6$, 8, and 10. In this case, even when using a three-term definition for $u_{\mathrm{LR}}(r)$, the leading contribution from the quadratic term in Eq. (6) would have an inverse power of 12,

$$V_{\mathrm{MLR}}(r) \simeq \mathcal{D}_e - \frac{C_6}{r^6} - \frac{C_8}{r^8} - \frac{C_{10}}{r^{10}} + \frac{(C_6)^2/(4\mathcal{D}_e)}{r^{12}} + \cdots, \tag{7}$$

and hence would not affect the limiting behavior defined by the chosen three-term $u_{\mathrm{LR}}(r)$ function.

In contrast, for a molecular state which dissociates to otherwise-identical S- and P-state atoms, the long-range potential would also include a $1/r^3$ term.[33,35] In this case, substituting the simple two-term definition $u_{\mathrm{LR}}(r)=C_3/r^3+C_6/r^6$ into Eq. (6) will yield the long-range behavior,

$$V_{\mathrm{MLR}}(r) \simeq \mathcal{D}_e - \frac{C_3}{r^3} - \frac{[C_6-(C_3)^2/(4\mathcal{D}_e)]}{r^6} + \frac{C_3C_6/(2\mathcal{D}_e)}{r^9} + \frac{(C_6)^2/(4\mathcal{D}_e)}{r^{12}}. \tag{8}$$

Thus, the quadratic term in Eq. (6) effectively introduces both a "fake" contribution to the overall $1/r^6$ behavior and unphysical repulsive $1/r^9$ and $1/r^{12}$ terms. The first is absolutely unacceptable, since the core of the model for this case requires the nonexponential part of the overall long-range potential to have the "true" specified $C_3/r^3+C_6/r^6$ leading terms, while the second is undesirable.

This problem can be addressed by defining $u_{\mathrm{LR}}(r)$ in a way which corrects for that modification of the effective C_6 value. In particular, if the C_6 coefficient in our expression for $u_{\mathrm{LR}}(r)$ is replaced by the "adjusted" value $C_6^{\mathrm{adj}}=C_6+(C_3)^2/(4\mathcal{D}_e)$, the coefficient of the $1/r^6$ term in the overall long-range tail of our MLR potential which includes the quadratic term in Eq. (6) will be simply the desired C_6 value. Similarly, the unphysical $1/r^9$ term will disappear from the

actual long-range potential of Eq. (8) if a compensating adjusted $1/r^9$ term is included in the definition of $u_{LR}(r)$ with the coefficient $C_9^{adj}=C_3C_6^{adj}/(2\mathfrak{D}_e)$. In this case, if $p=5$ the leading contribution due to the exponential term in the potential will actually have the form $-(A_5C_3)/r^8$, which has the radial behavior of the first theoretically predicted long-range term missing from our two-term definition of $u_{LR}(r)$.[28] Similarly, if a C_8/r^8 term is included in the definition of $u_{LR}(r)$ and we set $p=7$, this leading correction term will have the form $-(A_7C_3)/r^{10}$, which again has the form of the next dispersion contribution to the long-range potential for this system.[28]

Problems due to the quadratic term in Eq. (6) are most serious for cases in which the power of the leading long-range term in Eq. (5) is $m_1=3$, because the coefficient of the second term in the $u_{LR}(r)$ expansion is affected. However, these problems also arise for molecular ions, for which the leading contributions to the long-range potential usually[39] correspond to (inverse) powers $m=4$, 6, 8, and 10. In that case, if a three-term expression is used for $u_{LR}(r)$, the coefficient of its third term should be set as $C_8^{adj}=[C_8+(C_4)^2/(4\mathfrak{D}_e)]$ rather than the true C_8 value, while if a four-term expression is used, the coefficient of $1/r^{10}$ appearing in the definition of $u_{LR}(r)$ must be $C_{10}^{adj}=[C_{10}+C_4C_6/(2\mathfrak{D}_e)]$. Analogous adjusted coefficients would need to be incorporated in the $u_{LR}(r)$ expressions for molecules with $m_1=5$ and 6 if four or more terms are included in $u_{LR}(r)$. However, these problems will be encountered less frequently for cases with these higher m_1 values, because for most systems it is difficult to find/calculate estimates of the requisite high-order long-range coefficients which are reliable enough to justify use of such multiterm expressions.

2. The special case of $Li_2(A\ ^1\Sigma_u^+)$

It has long been known that for homonuclear dimers which dissociate to $M(ns\ ^2S)+M(np\ ^2P)$ atoms, a Hund's case (c) description is required at very large distances where the interaction energy is smaller than the atomic $n\ ^2P_{1/2}-n\ ^2P_{3/2}$ spin-orbit splitting energy, but a case (a) description is appropriate when the interaction energy is larger than that splitting.[40,41] As a result, the $0_u^+(A\ ^1\Sigma)$ state which dissociates to the (lower) $n\ ^2P_{1/2}+n\ ^2S_{1/2}$ limit and the $0_u^+(b\ ^3\Pi)$ state which dissociates to the (upper) $n\ ^2P_{3/2}+n\ ^2S_{1/2}$ limit interact at large distances where their potentials come close together. Aubert-Frécon (A-F) and co-workers[12,42] presented an analytic description of the radial behavior of such coupled states, which took account of the first-order resonance-dipole term, the leading dispersion energy terms, and the exchange energy. If we retain only the three longest-range terms and rewrite their expression for use in Eq. (1), we obtain

$$u_{LR}^{A\text{-}F}(r)=-\frac{A_{so}}{2}+\frac{C_3^\Sigma+C_3^\Pi}{2r^3}+\frac{C_6^\Sigma+C_6^\Pi}{2r^6}+\frac{C_8^\Sigma+C_8^\Pi}{2r^8}\pm\frac{1}{2}\left\{\left(\frac{C_3^\Sigma-C_3^\Pi}{3r^3}+\frac{C_6^\Sigma-C_6^\Pi}{3r^6}+\frac{C_8^\Sigma-C_8^\Pi}{3r^8}-A_{so}\right)^2+8\left(\frac{C_3^\Sigma-C_3^\Pi}{3r^3}+\frac{C_6^\Sigma-C_6^\Pi}{3r^6}+\frac{C_8^\Sigma-C_8^\Pi}{3r^8}\right)^2\right\}^{1/2},\qquad(9)$$

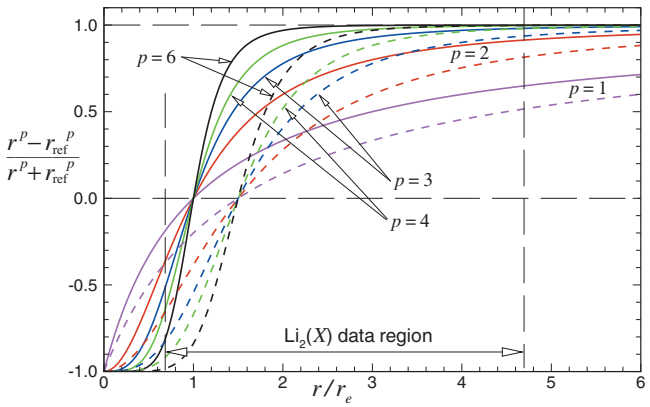

FIG. 2. Plot of the expansion variables [see Eq. (10)] $y_p^{eq}(r)=y_p(r;r_{ref}=r_e)$ (solid curves) and $y_p^{ref}(r)=y_p(r;r_{ref}=1.5r_e)$ (dashed curves) for various integer values of p, showing the data region for ground-state Li_2.

in which A_{so} is the (positive) difference between the $^2P_{1/2}$ and $^2P_{3/2}$ atomic spin-orbit levels, the "–" sign yields the $0_u^+(b\ ^3\Pi)$ state potential which approaches the upper $(^2P_{3/2})$ limit, and the "+" sign the $0_u^+(A\ ^1\Sigma^+)$ state potential which correlates with the lower $^2P_{1/2}$ atomic limit. This expression assumes the case (a) values of the various long-range potential coefficients $C_m^\Sigma\equiv C_m(^1\Sigma_u^+)$ and $C_m^\Pi\equiv C_m(^3\Pi_u)$. However, at this point we do not make use of the fact that $C_3^\Sigma=2C_3^\Pi$,[12,42] since the C_3^Σ and C_3^Π coefficients are modified in different ways by the effects of retardation (see Sec. IV B).[43,44] Note that in contrast with Refs. 12 and 42, the sign convention used in this paper is that positive C_n coefficients correspond to attractive contributions to the interaction potential.

Although this expression is somewhat complicated, it is a well-defined closed-form function of the parameters A_{so}, C_3^Σ, C_3^Π, C_6^Σ, C_6^Π, C_8^Σ, and C_8^Π. Hence, it is a straightforward matter to use it in Eq. (1) in place of the simple inverse-power series of Eq. (5). Of course, this cannot be done without taking account of the complications discussed in the preceding subsection. However, we will see below (in Sec. IVB) that in practice it is possible to neglect the effect of the $b\ ^3\Pi_u$ state dispersion coefficients C_6^Π and C_8^Π on the $A\ ^1\Sigma_u^+$-state potential.

3. Extending the definitions of $\beta(r)$ and $y_p(r)$

A problem associated with the use of $y_p^{eq}(r)$ as the expansion variable in Eq. (4) is illustrated by the solid curves in Fig. 2. As we see there, with increasing values of p the expansion variable of Eq. (3) [solid curves, denoted $y_p^{eq}(r)$] lie very close to the limiting value of +1 over an increasingly large fraction of the radial range sampled by the experimental data.[23] Over an interval within which $y_p^{eq}(r)$ changes very little, a relatively high-order polynomial expansion in that variable would be required to provide an accurate description of any function which is not almost constant there. Moreover, except for the very highest values of p, $y_p^{eq}(r)$ still differs significantly from the limiting value of -1 at the lower bound of the data region. As a result, a polynomial function of this variable yielding a potential which accurately reproduces the experimental data will still have ample opportunity to misbehave at distances less than the inner end of the data

region. Addressing this problem was the reason for introducing the use of different polynomial orders in Eq. (4) for $r < r_e$ and $r \geq r_e$.[27,31,45,46] However, that approach introduced its own problems, in that while polynomial coefficients β_i for $i \leq \min\{N_S, N_L\}$ usually have magnitudes of order ~ 1, β_i values for $i > \min\{N_S, N_L\}$ are often several orders of magnitude larger than that, and of oscillating sign (see e.g., Refs. 28 and 30). Moreover, as mentioned in Sec. III A, the use of orders $N_S \neq N_L$ introduces small discontinuities in high derivatives of the potential at r_e.

A simple solution to these problems is to express $\beta(r)$ in terms of a modified radial variable defined relative to a fixed reference distance r_{ref}, which is greater than r_e:

$$y_p^{\text{ref}}(r) \equiv y_p(r; r_{\text{ref}}) = \frac{r^p - r_{\text{ref}}^p}{r^p + r_{\text{ref}}^p}. \tag{10}$$

For the case $r_{\text{ref}} = 1.5 r_e$, the dashed curves in Fig. 2 show that this modified variable addresses both of the concerns raised above. In particular, for any given value of p, the onset of the region over which $y_p(r; r_{\text{ref}} = 1.5 r_e)$ becomes very flat and close to the +1 limit is pushed outward to substantially larger r, and the range of $y_p^{\text{ref}}(r)$ values associated with the data region becomes much more symmetric. As a result, for appropriate choices of r_{ref}, the powers N_S and N_L appearing in the definition of $\beta(r)$ in Eq. (4) may be set equal to one another, and achieving a given quality of fit will require lower-order polynomials than if $y_p^{\text{eq}}(r)$ were the expansion variable. Experience to date also shows that when this is done, the resulting expansion coefficients are all of roughly the same magnitude.

It is important to realize, however, that while use of $y_p^{\text{ref}}(r)$ as the expansion variable in Eq. (4) has many advantages, the algebraic structure of the MLR form means that the explicit factor of $y_p(r)$ appearing in the exponent must be $y_p^{\text{eq}}(r)$, yielding

$$V_{\text{MLR}}(r) = \mathcal{D}_e \left[1 - \frac{u_{\text{LR}}(r)}{u_{\text{LR}}(r_e)} e^{-\beta(r) \cdot y_p^{\text{eq}}(r)} \right]^2. \tag{11}$$

Independent of the value chosen for the (fixed) expansion center r_{ref} used in the definition of $\beta(r)$, this ensures that at $r = r_e$ the exponential term in Eq. (11) will equal 1, an essential feature of the MLR form.

One remaining question is how to choose an appropriate value for r_{ref}. Unfortunately there is no global answer, since the optimum value depends both on the range of the data and on the location of the onset of the region where the overall potential takes on the limiting behavior of Eq. (2) [or more correctly, of Eq. (6)]. However, experience to date suggests that trial-and-error fits using $r_{\text{ref}}/r_e \approx 1.1-1.5$ will quickly guide one to an optimum choice for r_{ref}.[47]

Introduction of the potential form of Eq. (11) with $r_{\text{ref}} > r_e$ and the associated simplification of fixing $N_S = N_L$ does allow one to attain more compact expansions than would be possible otherwise. However, for cases in which multiple long-range terms are included in the definition of $u_{\text{LR}}(r)$ (requiring p to be relatively large) and the turning points of the observed levels span a relatively large range of distances (e.g., extending to $r/r_e \gtrsim 3$), quite high-order exponent polynomials are still required to yield a potential energy function able to describe the system accurately. This occurs because the requirement[28] that $p > (m_{\text{last}} - m_1)$ means that at large r, the radial variable $y_p^{\text{ref}}(r)$ will still be relatively flat; e.g., see the dashed curve for $p=6$ in Fig. 2. However, a small additional modification of our definition of the exponent coefficient $\beta(r)$ addresses this remaining problem.

Examination of the asymptotic behavior of the exponential term in Eq. (1) shows that if we introduce a second radial variable $y_q^{\text{ref}}(r)$ defined in terms of some integer $q \neq p$ and rewrite $\beta(r)$ as

$$\beta(r) = \beta_p^q(r) \equiv y_p^{\text{ref}}(r) \beta_\infty + [1 - y_p^{\text{ref}}(r)] \sum_{i=0}^{N} \beta_i y_q^{\text{ref}}(r)^i, \tag{12}$$

the leading correction to the limiting value $(e^{-\beta_\infty})$ of that exponential involving the integer q has the form $A_{p,q}/r^{p+q}$. This means that the value of the power q used to define the radial variable in the explicit power series portion of this definition of $\beta_p^q(r)$ *does not affect* the nature of the "leading deviation" from the limiting asymptotic value of the exponential term in Eq. (1). This means that q may be given a relatively small value such as $q=2$, 3, or 4 without causing any distortion of the long-range tail of the potential implied by $u_{\text{LR}}(r)$. Use of one of these smaller values of q allows the behavior of $\beta_p^q(r)$ (and hence of the potential) to be described accurately by lower-order polynomials than would otherwise be required.

The two developments discussed in this section, (i) introduction of $r_{\text{ref}} > r_e$ and (ii) introduction of a separate power $q < p$, may seem very modest. However, they prove to be quite important in practice, as they allow for more compact potential function parametrization, and the resulting exponent expansion coefficients are much more weakly correlated. This leads to much more robust and reliable potential function forms.

IV. APPLICATION TO THE $A\,^1\Sigma_u^+ - X\,^1\Sigma_g^+$ SYSTEM OF Li_2

A. Data set used in the analysis

The experimental data set used in the present work is summarized in Table II. It is based on the very extensive data set used in the recent DPF analysis of this system reported by Coxon and Melville[24] (see their Table I), but incorporates a few noteworthy extensions. In particular, the present analysis includes the PAS data of Abraham *et al.*[1] which span A-state vibrational levels $v(A)=65-97$ for $^{7,7}Li_2$ and $v(A)=62-88$ for $^{6,6}Li_2$, the highest of which is bound by only 0.376 cm^{-1} and has an outer turning point of approximately 90 Å. In contrast, the highest A-state levels in the data set used by Coxon and Melville were $v(A)=62$ for $^{7,7}Li_2$ and $v(A)=84$, for $^{6,6}Li_2$, the latter being bound by 2.4 cm^{-1} and having an outer turning point of "only" 52 Å.

A second important extension is that the new measurements described in Sec. II include fluorescence transitions into high-v levels of A-state $^{7,7}Li_2$, so that these conventional data now span the range $v(A)=0-88$ [cf., $v(A)=0-62$ in Ref. 24]. In addition, a weak feature in the $^{6,6}Li_2$ fluores-

TABLE II. Summary of experimental data used in the present study.

Isotop.	Data Type	Unc. (cm^{-1})	$v(A)$	$v(X)$	No. of lines	Source
$^{7,7}Li_2$	$A-X$ bands	0.005–0.02	0–26	0–40	9086	Present, Refs. 9, 10, 14, and 15
	$A-X$ fluorescence	0.006	2, 3	0–11	1082	Ref. 15
	$E,F-A$ fluorescence	0.008–0.015	0–88	⋯	935	Present, Refs. 13 and 16
	PAS(A)	0.0007–0.008	66–97	⋯	55	Ref. 1
$^{6,6}Li_2$	$A-X$ bands	0.01 or 0.005	0–24	0–7	2911	Ref. 14 and 16
	$A-X$ fluorescence	0.005 or 0.006	0, 3, 5, 14, 22, 23	0–37	1936	Present, Ref. 15
	$E,F-A$ fluorescence	0.008	2–85	⋯	1056	Present, Refs. 11 and 16
	PAS(A)	0.0005–0.007	62–88	⋯	36	Ref. 1
$^{6,7}Li_2$	$A-X$ bands	0.005	0–5, 19	0–3, 25, 26	288	Present, Ref. 15
	$A-X$ fluorescence	0.005	19	9–33	46	Present
	$E-A$ fluorescence	0.008	34–71	⋯	45	Present
	PAS(A)	0.0007	83	⋯	1	Ref. 25

cence spectra has now been assigned as a transition to $v(A)=85$, which extends that data range by one vibrational quantum. These extensions are important because the overlap of the $E,F \rightarrow A$ fluorescence and PAS data ensure that the two types of data will be consistent with each other.

For the $X\,^1\Sigma_g^+$ state, an important extension of the present data set is the fact that new $A-X$ fluorescence measurements for $^{6,6}Li_2$ now extend to $v(X)=37$, a level with the same binding energy (1.99 cm^{-1}) as that for the highest observed vibrational level of $^{7,7}Li_2$ ($v(X)=40$). This is a significant change from the range $v(X)=0-14$ of the $^{6,6}Li_2$ data available to Coxon and Melville,[24] and it greatly improves our ability to delineate the "adiabatic" BOB radial strength function for this state in our combined isotopologue analysis. In addition to the extensions listed above, one other minor difference from the data set of Coxon and Melville[24] is that the 1986 $^{7,7}Li_2$ $A-X$ data of Barakat *et al.*[10] which were treated as fluorescence data in Ref. 24 are treated as band data in the present analysis, and hence provide information on the A state as well as on the X state.

Another significant feature of the present data set is a very considerable extension of the range of observed vibrational levels for the mixed isotopologue $^{6,7}Li_2$ in both the X and A states. The data for this species available to Coxon and Melville consisted of $A-X$ absorption bands spanning the ranges $v(X)=0-3$ and $v(A)=0-5$. However, recent experiments in Lyon yielded data for the (19, 25) and (19, 26) bands of the $A-X$ system in the form of rotational relaxation in an $A-X$ fluorescence series spanning levels $v''(X)=9-33$, and an $E-A$ fluorescence series covering levels $v(A)=34-71$ was discovered in the Lyon archives. The present data set also incorporates the PAS observation of level $v(A)=83$ of $^{6,7}Li_2$ reported by Schlöder *et al.*[25] As a result, the range of the data for the mixed isotopologue is now almost comparable to those for the much more extensively studied homonuclear species.

Except for the PAS datum of Ref. 25 (discussed later), the data uncertainties used in the present analysis were those estimated by the experimentalists. However, a modest number of lines for which the [calc.-obs.] values obtained from "good" fits were greater than four times the associated uncertainty were deweighted and omitted from the fit. The entire data set used in the present analysis is available as supplementary material from the journal's web archive.[48]

B. Potential energy functions

As mentioned in Sec. III A, for a molecule which dissociates to two S-state atoms, the leading terms in the long-range interaction potential have inverse powers $m=6$, 8, and 10, and if those are ground-state atoms, these dispersion energy terms are all attractive. This allows the long-range behavior of the potential to be defined by the simple sum of inverse power terms associated with the "basic MLR model" described in Sec. III A. Thus, the long-range behavior of the X-state potential may be defined using a two- or three-term version of the function

$$u_{\mathrm{LR}}^X(r) = \frac{C_6}{r^6} + \frac{C_8}{r^8} + \frac{C_{10}}{r^{10}}. \tag{13}$$

The values for the X-state dispersion energy coefficients used herein are fixed as those of Yan *et al.*,[49] which are considered[50] to be nearly "exact."

Our initial fits used the "basic MLR model" of Eq. (1) for the $X\,^1\Sigma_g^+$ state, with a two-term ($m_1=6$, $m_2=8$) expression for $u_{\mathrm{LR}}(r)$, with $p(=q)=4$, and with the exponent polynomial expressed in terms of y_p^{eq} (rather than y_p^{ref}). However, a relatively high-order exponent polynomial ($N_L \geq 21$ and $N_S \leq 7$) was required to achieve a fit matching experimental precision. Moreover, the resulting β_i expansion coefficients for $i > N_S$ were of oscillating sign and were up to ten orders of magnitude larger than coefficients of order $i \leq N_S$. This is a clear indication of a marginally stable model! In contrast, use of the extended version of the model represented by Eqs. (11) and (12) with the same two-term $u_{\mathrm{LR}}(r)$ function and $p=q=4$, but with $r_{\mathrm{ref}}=3.5$ Å ($\approx 1.3 r_e$), allowed us to obtain good fits with $N_S=N_L=17$, and the magnitudes of the associated expansion coefficients β_i typically differed from one another by less than a factor of ~ 100 (cf. by 10^{10}!). Furthermore, use of the generalized exponent coefficient expression of Eq. (12) with $q(=3)$ smaller than $p(=4)$ allowed an equally good fit to be achieved with $N(=N_S=N_L)=15$.[51] This comparison clearly demonstrates that the revised model

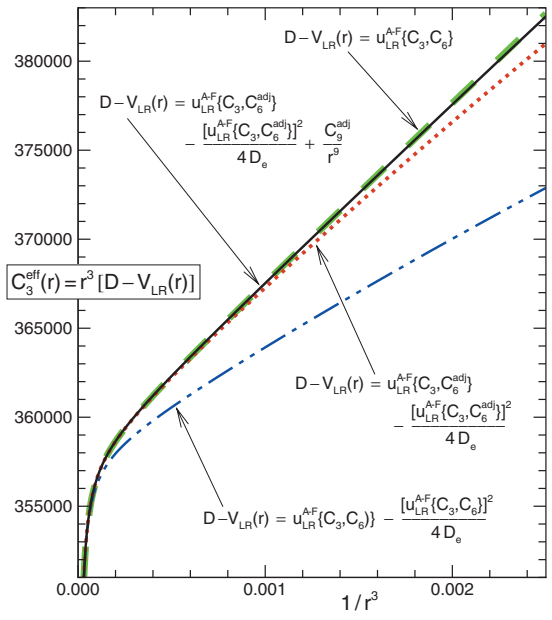

FIG. 3. Comparison of four representations of the long-range potential for the $A\ ^1\Sigma_u^+$ state of Li_2; energies are in cm^{-1} and distance in angstrom. As $1/r^3 \to 0$ all curves converge to the case (c) limiting value $(2/3)C_3^\Sigma$.

of Eqs. (11) and (12) with $r_{\text{ref}} > r_e$ and $q < p$ can yield much more compact, accurate potential energy function than may be obtained using the basic MLR model.

While it was convenient to use potentials based on a two-term $u_{\text{LR}}(r)$ function for the tests described above, the availability of accurate theoretical values of all three leading dispersion coefficients[49,50] invited the use of a more realistic model based on the three-term long-range potential of Eq. (13). This more severe constraint on the form of the long-range potential imposes the requirement that the exponent variable power p be ≥ 5.[28] However, trials showed that use of the extended MLR model of Eqs. (11) and (12) with exponent polynomial order of only $N=16$ yields an X-state potential able to accurately explain all of the data if $p=5$, $q=3$, and $r_{\text{ref}}=3.85$ Å. This is the form of our recommended model for the potential energy function of the $X\ ^1\Sigma_g^+$ state.

For the $A\ ^1\Sigma_u^+$ state we also used the extended MLR model of Eqs. (11) and (12), but its long-range behavior was based on the Aubert-Frécon expression of Eq. (9). The discussion of Sec. III B 1 shows that because its leading term is $\propto r^{-3}$ (whose square $\propto r^{-6}$), some adjustments are required. However, because of the complexity of this function and the fact that it involves two sets of long-range coefficients, C_m^Σ and C_m^Π, it seems appropriate to test the effectiveness of those modifications. To this end, Fig. 3 presents plots of $C_3^{\text{eff}}(r) \equiv r^3[\mathfrak{D} - V_{\text{LR}}(r)]$ for four different definitions of the long-range tail of the potential, $V_{\text{LR}}(r)$, all based in the long-range coefficients of Yan *et al.*,[49] but with the C_8^Σ and C_8^Π terms omitted for the sake of simplicity.

The thick green dashed curve in Fig. 3 shows the behavior of the function $r^3 u_{\text{LR}}^{\text{A-F}}(r)$ based on Eq. (9). This is the form of the actual long-range behavior we wish to incorporate in our model. In contrast, for $V_{\text{LR}}(r) = \mathfrak{D} - C_3/r^3 - C_6/r^6$, the plot in Fig. 3 would be a straight line with intercept C_3 and slope C_6. It is clear that at very large distances ($1/r^3 \lesssim 0.0002$ Å^{-3}), the simple linear extrapolation to an intercept of $C_3^\Sigma = 3.577\,58 \times 10^5$ cm^{-1} Å^3 is interrupted by the change from Hund's case (a) to case (c) coupling. The blue dash-dot-dot curve in Fig. 3 shows the effect on this predicted long-range potential of including the quadratic term which Eq. (6) shows is an implicit part of the MLR form. The red dotted curve then shows how this long-range behavior is corrected if we replace C_6^Σ in our expression for $u_{\text{LR}}^{\text{A-F}}(r)$ by

$$C_6^{\text{adj}} = C_6^\Sigma + \frac{(C_3^\Sigma)^2}{4\mathfrak{D}_e}. \tag{14}$$

Finally, the solid black curve shows that if the term C_9^{adj}/r^9 is added to this expression, where

$$C_9^{\text{adj}} = \frac{C_3^\Sigma C_6^{\text{adj}}}{2\mathfrak{D}_e} = \frac{C_3^\Sigma C_6^\Sigma}{2\mathfrak{D}_e} + \frac{(C_3^\Sigma)^3}{8(\mathfrak{D}_e)^2}, \tag{15}$$

we obtain very close agreement with the desired long-range form over the whole range spanned by this diagram ($r \gtrsim 7.4$ Å).

The modifications described above involve replacing C_6^Σ by C_6^{adj} and introducing C_9^{adj}, but ignore the coefficient C_6^Π, although the latter also appears in the general $u_{\text{LR}}^{\text{A-F}}(r)$ expression of Eq. (9) and theory predicts that $C_6^\Pi/C_6^\Sigma \approx 0.68$.[49] This neglect is appropriate because defining C_6^Π by the above ratio or setting it to zero has no significant effect on the quality of fit or fitted potential parameters, and no discernible effect on any of the curves seen in Fig. 3. This may be understood if we examine the behavior of $V_{\text{LR}}(r) = \mathfrak{D} - u_{\text{LR}}^{\text{A-F}}(r)$ in the two domains: A_{so} greater than, versus A_{so} less than the terms $[(C_3^\Sigma - C_3^\Pi)/(3r^3) + (C_6^\Sigma - C_6^\Pi)/(3r^6) + \cdots]$ appearing under the square root signs in Eq. (9). In particular, at intermediate r where A_{so} is small compared to this sum, the leading contributions from C_3^Π, C_6^Π, and C_8^Π completely cancel out, yielding

$$V_{\text{LR}}(r) \approx \mathfrak{D} + \frac{2}{3}A_{\text{so}} - \frac{C_3^\Sigma}{r^3} - \frac{C_6^\Sigma}{r^6} - \frac{C_8^\Sigma}{r^8} + \mathcal{O}\left(\frac{A_{\text{so}}^2}{C_3^\Sigma/r^3}\right). \tag{16}$$

This shows that if the potential was determined mainly by data for levels with outer turning points at distances $r \lesssim 14$ Å (i.e., $r^{-3} \gtrsim 0.0004$ in Fig. 3), it would tend to dissociate to the nonphysical limit of the weighted average of the $^2P_{1/2}$ and $^2P_{3/2}$ energy asymptotes, rather than to the actual (lower) $^2P_{1/2}$ limit at energy $\mathfrak{D}$. This was the case for the analyses reported in Refs. 11 and 24.

At the very large distances where A_{so} is larger than the sum of inverse-power terms under the square root sign in Eq. (9), the long-range potential becomes (utilizing the identity $C_3^\Pi = C_3^\Sigma/2$)

$$V_{\text{LR}}(r) \approx \mathfrak{D} - \frac{2}{3}\frac{C_3^\Sigma}{r^3} - \frac{1}{r^6}\left\{\frac{(C_3^\Sigma)^2}{18A_{\text{so}}} + \frac{C_6^\Sigma + 2C_6^\Pi}{3} - \frac{(C_3^\Sigma)^2}{12\mathfrak{D}_e}\right\} + \mathcal{O}(r^{-8}). \tag{17}$$

Equation (17) shows that in the limit of very large r the potential dies off as $1/r^3$ and approaches the (lower) $^2P_{1/2}$ asymptote with a case (c) C_3 coefficient which is precisely 2/3 of the case (a) C_3^Σ value. This case (c) C_3 value is the

actual intercept of all of the curves shown in Fig. 3. Moreover, the coefficient of $1/r^6$ in this expression is totally dominated by the term $(C_3^{\Sigma})^2/(18A_{so})$, with the $(C_6^{\Sigma}+2C_6^{\Pi})$ term making less than a 0.04% contribution to its magnitude. Since the overall interaction energy in this region is <0.2 cm^{-1}, most of which is due to the C_3 term, this contribution will have a negligible effect on the energies of observed levels. Thus, Eqs. (16) and (17) explain our empirical finding that the contribution of the coefficients C_6^{Π} and C_8^{Π} to the long-range potential for the $A\ ^1\Sigma_u^+$ state of Li_2 can be neglected.

One final point which must be considered is the fact that at the relatively large distances where the C_3/r^3 term comes to dominate the interaction, "retardation" effects due to the finite speed of light cannot be neglected. It has long been known[43,44] that the effect of retardation on an s/p resonance dipole interaction can be accounted for by replacing C_3^{Σ} by $C_3^{\Sigma,\mathrm{ret}}=C_3^{\Sigma}f_{\mathrm{ret}}^{\Sigma}$ and C_3^{Π} by $C_3^{\Pi,\mathrm{ret}}=C_3^{\Pi}f_{\mathrm{ret}}^{\Pi}$, where[44]

$$f_{\mathrm{ret}}^{\Sigma}=\cos\left(\frac{2\pi r}{\lambda_{SP}}\right)+\left(\frac{2\pi r}{\lambda_{SP}}\right)\sin\left(\frac{2\pi r}{\lambda_{SP}}\right), \tag{18}$$

$$f_{\mathrm{ret}}^{\Pi}=f_{\mathrm{ret}}^{\Sigma}-\left(\frac{2\pi r}{\lambda_{SP}}\right)^2\cos\left(\frac{2\pi r}{\lambda_{SP}}\right), \tag{19}$$

and λ_{SP} is the wavelength of light associated with the atomic $^2S-^2P$ transition. It is a straightforward matter to utilize this substitution in Eq. (9).

The above considerations indicate that the long-range form of an MLR potential for the $A\ ^1\Sigma_u^+$ state of Li_2 should be defined by the function

$$u_{\mathrm{LR}}^{A,\mathrm{ret}}(r)=-\frac{A_{so}}{2}+\frac{C_3^{\Sigma}f_{\mathrm{ret}}^{+}}{2r^3}+\frac{C_6^{\mathrm{adj}}}{2r^6}+\frac{C_8^{\Sigma}}{2r^8}+\frac{C_9^{\mathrm{adj}}}{r^9}+\frac{1}{2}\left\{\left(\frac{C_3^{\Sigma}f_{\mathrm{ret}}^{-}}{3r^3}+\frac{C_6^{\mathrm{adj}}}{3r^6}+\frac{C_8^{\Sigma}}{3r^8}-A_{so}\right)^2+8\left(\frac{C_3^{\Sigma}f_{\mathrm{ret}}^{-}}{3r^3}+\frac{C_6^{\mathrm{adj}}}{3r^6}+\frac{C_8^{\Sigma}}{3r^8}\right)^2\right\}^{1/2}, \tag{20}$$

in which $f_{\mathrm{ret}}^{\pm}=f_{\mathrm{ret}}^{\Sigma}\pm\frac{1}{2}f_{\mathrm{ret}}^{\Pi}$, C_6^{adj} and C_9^{adj} are defined by Eqs. (14) and (15), and we have now utilized the fact that $C_3^{\Pi}=C_3^{\Sigma}/2$.[12,42] These retardation functions vary quite modestly across the data region: for example, $f_{\mathrm{ret}}^{\Sigma}(r)=1.000\ 04$ at $r=10$ Å, 1.0011 at $r=50$ Å, 1.0044 at $r=100$ Å, and 1.0098 at $r=150$ Å. However, this variation does have a significant effect on the value of C_3^{Σ} determined from our analysis.

Finally, the normal MLR-function requirement that $p>(m_{\mathrm{last}}-m_1)=8-3=5$ led us to set $p=6$ for the A-state MLR potential, while tests showed that setting $q=3$ and $r_{\mathrm{ref}}=4.4$ Å allowed us to obtain an excellent fit to the data using a compact exponent expansion order of only $N=16$. Together with the use of Eq. (20) to define $u_{\mathrm{LR}}(r)$ in Eq. (11), this defines the form of the MLR potential for the $A\ ^1\Sigma_u^+$ state of Li_2 used in the final stage of our analysis. However, the formulation up to this point neglects the BOB effects which give rise to differences between the effective potentials for different isotopologues of a given species. For the $A\ ^1\Sigma_u^+$ state of Li_2, this also leads to the inclusion an additional term in the definition of the total effective adiabatic potential.

C. Born–Oppenheimer breakdown functions

In combined-isotopologue analyses of high resolution data, it is almost always necessary to take account of the BOB effects which give rise to small differences between the rotationless potentials for different isotopologues, and to small atomic-mass-dependent contributions to the rotational level energies. Such effects are especially important for diatomics containing at least one light atom. Following established formalisms,[52–54] the vibration-rotation levels of isotopologue α of diatomic molecule A-B in a given electronic state are the eigenvalues of the radial Schrödinger equation

$$\left\{-\frac{\hbar^2}{2\mu_\alpha}\frac{d^2}{dr^2}+[V_{\mathrm{ad}}^{(1)}(r)+\Delta V_{\mathrm{ad}}^{(\alpha)}(r)]+\frac{\hbar^2J(J+1)}{2\mu_\alpha r^2}[1+g^{(\alpha)}(r)]\right\}\psi_{v,J}(r)=E_{v,J}\psi_{v,J}(r), \tag{21}$$

in which $V_{\mathrm{ad}}^{(1)}(r)$ is the effective adiabatic interaction potential for a selected reference isotopologue labeled $\alpha=1$, $\Delta V_{\mathrm{ad}}^{(\alpha)}(r)=V_{\mathrm{ad}}^{(\alpha)}(r)-V_{\mathrm{ad}}^{(1)}(r)$ is the *difference* between the effective adiabatic potentials for isotopologue-α and isotopologue-1, $g^{(\alpha)}(r)$ is the nonadiabatic centrifugal-potential correction function for isotopologue-α, and the reduced mass μ_α is defined by the atomic masses $M_{\mathrm{A}}^{(\alpha)}$ and $M_{\mathrm{B}}^{(\alpha)}$. Following standard conventions,[31,45,52–54] the BOB terms $\Delta V_{\mathrm{ad}}^{(\alpha)}(r)$ and $g^{(\alpha)}(r)$ are each written as a sum of contributions from the two component atoms Li(A) and Li(B). In the present homopolar molecule case these expressions collapse to

$$\Delta V_{\mathrm{ad}}^{(\alpha)}(r)=\left(\frac{\Delta M_{\mathrm{Li(A)}}^{(\alpha)}}{M_{\mathrm{Li(A)}}^{(\alpha)}}+\frac{\Delta M_{\mathrm{Li(B)}}^{(\alpha)}}{M_{\mathrm{Li(B)}}^{(\alpha)}}\right)\tilde{S}_{\mathrm{ad}}^{\mathrm{Li}}(r), \tag{22}$$

$$g^{(\alpha)}(r)=\left(\frac{M_{\mathrm{Li(A)}}^{(1)}}{M_{\mathrm{Li(A)}}^{(\alpha)}}+\frac{M_{\mathrm{Li(B)}}^{(1)}}{M_{\mathrm{Li(B)}}^{(\alpha)}}\right)\tilde{R}_{\mathrm{na}}^{\mathrm{Li}}(r), \tag{23}$$

where $\Delta M_{\mathrm{Li(A/B)}}^{(\alpha)}=M_{\mathrm{Li(A/B)}}^{(\alpha)}-M_{\mathrm{Li(A/B)}}^{(1)}$ are the differences between the atomic masses of lithium atoms A and B in isotopologue-α and in isotopologue-1. Note that although there is only a single radial strength function of each type, $\tilde{S}_{\mathrm{ad}}^{\mathrm{Li}}(r)$ and $\tilde{R}_{\mathrm{na}}^{\mathrm{Li}}(r)$, two mass factors must be retained in order to describe all three molecular isotopologues.

As for $\beta(r)$, the radial strength functions in Eqs. (22) and (23) are expressed as polynomials constrained to have specified asymptotic values:

$$\tilde{S}_{\mathrm{ad}}^{\mathrm{Li}}(r)=y_{p_{\mathrm{ad}}}^{\mathrm{eq}}(r)u_\infty^{\mathrm{Li}}+[1-y_{p_{\mathrm{ad}}}^{\mathrm{eq}}(r)]\sum_{i=0}u_i^{\mathrm{Li}}y_{q_{\mathrm{ad}}}^{\mathrm{eq}}(r)^i, \tag{24}$$

$$\tilde{R}_{\mathrm{na}}^{\mathrm{Li}}(r)=y_{p_{\mathrm{na}}}^{\mathrm{eq}}(r)t_\infty^{\mathrm{Li}}+[1-y_{p_{\mathrm{na}}}^{\mathrm{eq}}(r)]\sum_{i=0}t_i^{\mathrm{Li}}y_{q_{\mathrm{na}}}^{\mathrm{eq}}(r)^i, \tag{25}$$

in which u_∞^{Li} and t_∞^{Li} are the values of these functions in the limit $r\to\infty$, and u_0^{Li} and t_0^{Li} define their values at $r=r_e$.[45] The discussion of Ref. 45 shows that $t_\infty^{\mathrm{A}}=0.0$ for any molecule which dissociates to yield an uncharged atom A, so $t_\infty^{\mathrm{Li}}(X\ ^1\Sigma_g^+)=t_\infty^{\mathrm{Li}}(A\ ^1\Sigma_u^+)=0.0$. In addition, we adopt the Watson convention of setting the parameter $t_0^{\mathrm{Li}}=0.0$ for both the X and A states, since its value cannot be determined from transition-frequency data alone.[45,52,53]

It is of course necessary to specify the powers $p_{\rm ad}$, $q_{\rm ad}$, $p_{\rm na}$, and $q_{\rm na}$ defining the radial expansion variables in Eqs. (24) and (25). As was pointed out in Ref. 54, if the effective adiabatic potential for the "minor" isotopologues is to have the same limiting long-range behavior as that for isotopologue-1, $p_{\rm ad}$ must be equal to or greater than the power of the longest-range term in the intermolecular potential for that state. We therefore set $p_{\rm ad}(X\ ^1\Sigma_g^+)=6$ and $p_{\rm ad}(A\ ^1\Sigma_u^+)=3$. Since these radial strength functions are relatively weak, few terms are required to define them, and there is no need to introduce an $r_{\rm ref}\neq r_e$ extension into the definition of the expansion variables in Eqs. (24) and (25).

We are not aware of any theoretical predictions regarding the limiting long-range behavior of the centrifugal nonadiabatic radial strength function $\tilde{R}^A_{\rm na}(r)$, so we have no basis for assigning particular values to $p_{\rm na}$. Moreover, as in the case of the MLR exponent coefficient expression (12), there are no physical constraints on the values of $q_{\rm ad}$ or $q_{\rm na}$. At the same time, Fig. 3 of Ref. 45 shows that use of too small values for these powers can give rise to physically implausible extrema in the resulting functions on the interval between the data region and the asymptote, while the behavior seen in Fig. 2 indicates that use of too high values will lead to a requirement for an excessive number of expansion coefficients. In the present work we chose to set $q_{\rm ad}=6(=p_{\rm ad})$ for the $X\ ^1\Sigma_g^+$ state and $q_{\rm ad}=p_{\rm ad}=p_{\rm na}=q_{\rm na}=3$ for the $A\ ^1\Sigma_u^+$ state. It was not necessary to specify $p_{\rm na}$ or $q_{\rm na}$ for the $X\ ^1\Sigma_g^+$ state, since our analysis showed that no centrifugal BOB terms for the $X\ ^1\Sigma_g^+$ state could be determined from the available data.

The discussion of Ref. 54 pointed out that the asymptotic value of an adiabatic radial strength function $\tilde{S}^A_{\rm ad}(r)$ should be consistent with the relevant atomic isotope shift. Following the convention of Ref. 54, the absolute zero of energy is defined herein as being the energy of all ground-state atomic isotopes separated at $r\to\infty$, so by definition $u^{\rm Li}_\infty(X\ ^1\Sigma_g^+)=0.0$. Since the $A\ ^1\Sigma_u^+$ state of Li_2 dissociates to one ground-state ($^2S_{1/2}$) and one excited-state ($^2P_{1/2}$) atom, the value of $u^{\rm Li}_\infty(A)\ ^1\Sigma_u^+)$ is then defined[54] by the difference between the atomic $^2P_{1/2}\leftarrow{}^2S_{1/2}$ excitation energies for ^{6}Li and ^{7}Li:[6]

$$\delta E^{^6{\rm Li}}_{^7{\rm Li}}(^2P_{1/2}) = \Delta E^{^6{\rm Li}}(^2P_{1/2}\leftarrow{}^2S_{1/2}) - \Delta E^{^7{\rm Li}}(^2P_{1/2}\leftarrow{}^2S_{1/2}) = -0.351\ 338\ [{\rm cm}^{-1}]. \quad (26)$$

As seen in Fig. 4, this is the difference between the asymptotes of the A-state potentials of $^{6,6}Li_2$ and $^{7,7}Li_2$, and it determines the asymptotic value of the radial strength function $\tilde{S}^{\rm Li}_{\rm ad}(r)$.[54] In particular, since we select $^{7,7}Li_2$ as the reference isotopologue,

$$u^{\rm Li}_\infty(A\ ^1\Sigma_u^+) = \delta E^{^6{\rm Li}}_{^7{\rm Li}}(^2P_{1/2})/2\left(1-\frac{M(^7{\rm Li})}{M(^6{\rm Li})}\right) = 1.055\ 74\ [{\rm cm}^{-1}]. \quad (27)$$

Since $y^{\rm eq}_{p_{\rm ad}}(r_e)=0$ and $y^{\rm eq}_{p_{\rm ad}}(r\to\infty)=1$, the algebraic form of Eqs. (22) and (24) means that $\Delta V^{(\alpha)}_{\rm ad}(r)$ gives rise to difference between the well depths and equilibrium distances for different Li_2 isotopologues in a given electronic state,[56,57]

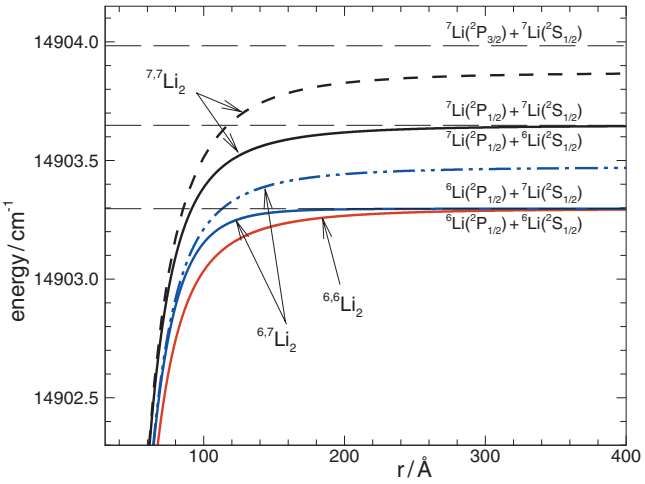

FIG. 4. Solid curves: long-range behavior of our recommended A-state potentials for $^{7,7}Li_2$ (black, uppermost solid curve), for $^{6,6}Li_2$ (red, lowest solid curve), and for $^{6,7}Li_2$ (blue, intermediate solid curve). Dashed black curve: Long-range behavior of the A-state potential for $^{7,7}Li_2$ if spin-orbit induced interstate mixing is ignored. Dash-dot-dot blue curve: long-range behavior of the A-state potential for $^{6,7}Li_2$ if the g/u symmetry breakdown is ignored.

$$\delta\mathfrak{D}^{(\alpha)}_e = \mathfrak{D}^{(\alpha)}_e - \mathfrak{D}^{(1)}_e = \left(\frac{\Delta M^{(\alpha)}_{\rm Li(A)}}{M^{(\alpha)}_{\rm Li(A)}} + \frac{\Delta M^{(\alpha)}_{\rm Li(B)}}{M^{(\alpha)}_{\rm Li(B)}}\right)(u^{\rm Li}_\infty - u^{\rm Li}_0), \quad (28)$$

$$\delta r^{(\alpha)}_e = r^{(\alpha)}_e - r^{(1)}_e = -\left(\frac{\Delta M^{(\alpha)}_{\rm Li(A)}}{M^{(\alpha)}_{\rm Li(A)}} + \frac{\Delta M^{(\alpha)}_{\rm Li(B)}}{M^{(\alpha)}_{\rm Li(B)}}\right)\frac{\tilde{S}'_{\rm ad}(r_e)}{\bar{k}}, \quad (29)$$

in which $\bar{k}$ is the harmonic force constant at the potential minimum in units cm^{-1} Å^{-2}, and

$$\tilde{S}'_{\rm ad}(r_e) \equiv \left(\frac{d\tilde{S}_{\rm ad}}{dr}\right)_{r=r_e} = \frac{(u_\infty - u_0)p_{\rm ad} + u_1 q_{\rm ad}}{2r_e}. \quad (30)$$

These expressions apply to our description of the $X\ ^1\Sigma_g^+$ state. However, an additional BOB term gives rise to additional contributions to these isotope shifts the $A\ ^1\Sigma_u^+$ state.

Up to this point the discussion in this section has been generic, and would apply to the a multi-isotopologue description of any homonuclear diatomic. However, McAlexander *et al.*[4] pointed out that for the $A\ ^1\Sigma_u^+$ state of Li_2, the dominant BOB contribution to the rotationless potential at large r has the form

$$\Delta V^A_{\rm na}(r) = 2B^{(\alpha)}(r) = 2\left(\frac{\hbar^2}{2\mu_\alpha r^2}\right), \quad (31)$$

and since μ_α for isotopic Li_2 is relatively small, this behavior cannot be neglected. Efforts to incorporate this term into our definition of $u_{\rm LR}(r)$ were unsatisfactory because the complexity of the associated changes in the form of $\Delta V^{(\alpha)}_{\rm ad}(r)$ made that approach unwieldy. We therefore followed McAlexander *et al.*[4] and treated it as a separate additive contribution to the potential. As a result, our total effective adiabatic potential for isotopologue α in the $A\ ^1\Sigma_u^+$ state is written as

$$V^{(\alpha)}_{\rm ad,tot}(r) = V^{(1)}_{\rm ad,MLR}(r) + \Delta V^{(\alpha)}_{\rm ad}(r) + 2B^{(\alpha)}(r). \quad (32)$$

As was pointed out by Vogt *et al.*,[55] this $\Delta V_{\rm na}^{A}(r)$ term is readily incorporated into the Hamiltonian by simply replacing the factor $[J(J+1)]$ in Eq. (21) by $[J(J+1)+2]$. However, it also means that the overall A-state well depth and equilibrium distance become $\mathfrak{D}_e^{\rm tot}(A)=\mathfrak{D}_e^{(\alpha)}-2B^{(\alpha)}(r_e)$ and $r_e^{\rm tot}(A)=r_e^{(\alpha)}+4B^{(\alpha)}(r_e)/(\bar{k}r_e)$, where $\mathfrak{D}_e^{(\alpha)}$ and $r_e^{(\alpha)}$ are defined by Eqs. (28) and (29), and $\mathfrak{D}_e^{(1)}$ and $r_e^{(1)}$ are the (fitted) reference-isotopologue MLR parameters for that state. This in turn gives rise to additional contributions to the isotopic shifts of the well depth and equilibrium distance for this state. In particular,

$$\delta\mathfrak{D}_{e,\rm tot}^{(\alpha)}(A)=\delta\mathfrak{D}_e^{(\alpha)}-\frac{\hbar^2}{(r_e)^2}\left(\frac{1}{\mu_\alpha}-\frac{1}{\mu_1}\right), \tag{33}$$

$$\delta r_{e,\rm tot}^{(\alpha)}(A)=\delta r_e^{(\alpha)}+\frac{2\hbar^2/(r_e)^3}{\bar{k}}\left(\frac{1}{\mu_\alpha}-\frac{1}{\mu_1}\right), \tag{34}$$

in which $\delta\mathfrak{D}_e^{(\alpha)}$ and $\delta_e^{(\alpha)}$ are defined by Eqs. (28) and (29). Similarly, the electronic isotope shift for states A and X may be written as

$$\begin{aligned}\Delta T_e^{(\alpha)}(A\leftarrow X)&=T_e^{(\alpha)}(A\leftarrow X)-T_e^{(1)}(A\leftarrow X)\\&=\left(\frac{\Delta M_{{\rm Li}^a}^{(\alpha)}}{M_{{\rm Li}^a}^{(\alpha)}}+\frac{\Delta M_{{\rm Li}^b}^{(\alpha)}}{M_{{\rm Li}^b}^{(\alpha)}}\right)[u_0^{\rm Li}(A)-u_0^{\rm Li}(X)]\\&\quad+\frac{\hbar^2}{(r_e^A)^2}\left(\frac{1}{\mu_\alpha}-\frac{1}{\mu_1}\right).\end{aligned} \tag{35}$$

D. Effect of the disappearance of g/u symmetry for $^{6,7}Li_2$

The approach described above for defining the limiting value of the adiabatic radial strength functions $\tilde{S}_{\rm ad}^{A}(r)$ is appropriate for excited states of heteropolar diatomic molecules $(A\neq B)$ and for homonuclear molecules such as $^{6,6}Li_2$ and $^{7,7}Li_2$. However, it does not work for heteronuclear homopolar molecules such as $^{6,7}Li_2(A\ ^1\Sigma_u^+)$ which dissociate to an excited-atom asymptote. In particular, the Eq. (27) definition for $u_\infty^{\rm Li}$ would take the effective potential for the mixed isotopologue to a nonphysical limit half-way between the two physical asymptotes, $^6{\rm Li}(^2P_{1/2})+^7{\rm Li}(^2S_{1/2})$ or $^6{\rm Li}(^2S_{1/2})+^7{\rm Li}(^2P_{1/2})$, instead of to one or the other, as illustrated by the blue dot-dot-dash curve in Fig. 4.

Our treatment of this problem is based on the approach de Lange *et al.* used to take account of g/u symmetry breakdown in a state of HD which dissociates yield $H(2p)+D(1s)$.[58,59] They pointed out that as the interaction energy dies off at large r, when its magnitude approaches that of the spacing between the $H(2p)+D(1s)$ and $H(1s)+D(2p)$ asymptotes, the resonance dipole-dipole interaction term disappears, and the effective potential becomes dominated by the leading dispersion term (C_6/r^6) and approaches the lower of those asymptotes, $H(2p)+D(1s)$. For HD the 22.35 cm^{-1} spacing between the two isotopic limits is almost two orders of magnitude larger than the 0.36 cm^{-1} $^2P_{1/2}-^2P_{3/2}$ spin-orbit splitting, so the latter was ignored. In contrast, in the present case those two splittings have very similar magnitudes of 0.335 and 0.351 cm^{-1}, so a proper description would require a four-state treatment.

Fortunately, since the highest observed level of $^{6,7}Li_2(A\ ^1\Sigma_u^+)$ lies more than 6 cm^{-1} below dissociation, an approximate treatment of the g/u isotopic symmetry breaking will suffice here. In particular, in the spirit of the approach of de Lange *et al.*,[58,59] we represent the effect of the g/u symmetry breaking on the long-range potential of $^{6,7}Li_2(A\ ^1\Sigma_u^+)$ by including the difference between the leading long-range inverse-power term and the diagonalized coupling interaction,

$$dV_{g/u}^{(6,7)}(r)=\frac{C_3}{r^3}-\sqrt{\left(\frac{C_3}{r^3}\right)^2+\left(\frac{\delta E_{^7{\rm Li}}^{^6{\rm Li}}(^2P_{1/2})}{2}\right)^2}, \tag{36}$$

as an additive correction to the overall effective adiabatic potential for the mixed isotopologue. Since we are mainly concerned with providing a realistic extrapolation to the correct asymptote, we use the limiting case (c) value of the resonance dipole-dipole interaction coefficient, $C_3=(2/3)C_3^{\Sigma}$. As is shown by the solid blue curve for $^{6,7}Li_2$ in Fig. 4, inclusion of this term causes the effective adiabatic potential for $^{6,7}Li_2(A\ ^1\Sigma_g^+)$ to approach the correct (lower) physical limit of $^6{\rm Li}(^2P_{1/2})+^7{\rm Li}(^2S_{1/2})$ with $1/r^6$ limiting functional behavior.

E. Results

1. Choice of model and the resulting potentials

The present analysis of the $A-X$ system of Li_2 was performed using program DPOTFIT,[60] which incorporates all aspects of the potential energy and BOB function models discussed above, and can readily treat experimental data of all relevant types. As in any DPF analysis, the program solves Eq. (21) for the upper and lower level of each transition, uses the resulting wave functions to calculate partial derivatives of the eigenvalues with respect to every parameter in the model, and then uses an iterative nonlinear least-squares procedure to optimize the parameters defining the potential energy and BOB functions. As in any nonlinear least-squares procedure, this requires plausible initial trial values of the fitting parameters. For the potential energy functions such trial parameters are readily obtained by fitting *ab initio* potential energies, RKR turning points obtained from a traditional "parameter-fit" analysis, or turning points obtained from an earlier DPF fit, to the chosen analytic functional form. This was done using program BETAFIT.[61] Once a potential has been determined from a fit to data for a single isotopologue, combined-isotopologue fits can proceed from that potential with initial trial values of all BOB parameters being zero.

The parameters defining our final recommended potentials and BOB radial strength functions for the $X\ ^1\Sigma_g^+$ and $A\ ^1\Sigma_u^+$ states of Li_2 are presented in Table III. They were obtained from a fit to the 17 477 data summarized in Table II,

TABLE III. Parameters defining the recommended MLR potentials and BOB functions for the $X\ ^1\Sigma_g^+$ and $A\ ^1\Sigma_u^+$ states of Li_2 with $^{7,7}Li_2$ as the reference isotopologue. The analysis used the $^7Li\ ^2P_{1/2} \leftarrow 2S_{1/2}$ excitation energy of 14 903.648 130 cm^{-1} and $^2P_{3/2} \leftarrow 2P_{1/2}$ spin-orbit splitting energy of 0.335 338 cm^{-1} (Ref. 6). Units of length and energy are angstrom and cm^{-1}; the exponent expansion coefficients β_i and the centrifugal BOB parameters t_i of Eq. (25) are dimensionless, while the parameters u_i defining the "adiabatic" BOB strength function of Eq. (24) have units of cm^{-1}.

	$X\ ^1\Sigma_g^+$		$A\ ^1\Sigma_u^+$
$\mathfrak{D}_e$	8516.709 (4)		9353.167 (4)
r_e	2.672 993 (2)		3.107 856 (5)
C_6	$[6.715\ 27 \times 10^6]$	C_3^Σ	$3.578\ 29\ (8) \times 10^5$
C_8	$[1.125\ 88 \times 10^8]$	C_6^Σ	$[1.000\ 045 \times 10^7]$
C_{10}	$[2.786\ 04 \times 10^9]$	C_8^Σ	$[3.7020 \times 10^8]$
$\{p,q\}$	{5, 3}		{6, 3}
r_{ref}	[3.85]		[4.4]
β_0	−2.898 287 01		−1.757 832 35
β_1	−1.309 265		−1.034 889
β_2	−2.018 507		−1.811 924
β_3	−1.381 62		−1.623 41
β_4	−1.219 33		−1.443 47
β_5	0.3463		1.239 78
β_6	0.1061		2.9415
β_7	−0.1886		2.4661
β_8	1.671		1.9912
β_9	10.943		16.947
β_{10}	3.944		20.506
β_{11}	−27.23		−28.26
β_{12}	−11.49		−55.65
β_{13}	56.7		9.68
β_{14}	38.9		46.1
β_{15}	−37.4		2.0
β_{16}	−33.0		−14.3
$\{p_{ad},q_{ad}\}$	{6, 6}		{3, 3}
u_0	0.194 (10)		1.066 (10)
u_1	−0.01 (16)		2.98 (31)
u_2	0.39 (7)		−0.32 (26)
u_3	⋯		2.3 (10)
u_4	⋯		−7.5 (10)
u_5	⋯		3.3 (10)
u_∞	[0.0]		[1.055 740]
$\{p_{na},q_{na}\}$	⋯		{3, 3}
t_0	⋯		[0.0]
t_1	⋯		0.000 092 (9)
t_∞	⋯		[0.0]

and yielded a dimensionless rms deviation of $\overline{dd}=1.0059$. The compact form of these parameters reflects our use of the sequential rounding and refitting procedure of Ref. 62, which is a standard option in program DPOTFIT.[60] Parameters held fixed in the fits are shown in square brackets, while numbers in parentheses are the correlated 95% confidence limit uncertainties in the last digits shown for parameters with some direct physical significance. The three dispersion coefficients for the ground $X\ ^1\Sigma_g^+$ state and C_6^Σ for the $A\ ^1\Sigma_u^+$ state were fixed at values reported by Yan *et al.*,[49] while the value of C_8^Σ for the $A\ ^1\Sigma_u^+$ state was taken from Zhang *et al.*[50] In addition to the explicit parameters of the model, our description of this system relies on the $^2P_{1/2} \leftarrow {}^2S_{1/2}$ and $^2P_{3/2} \leftarrow {}^2S_{1/2}$ excitation energies of ^7Li and ^6Li reported by Sansonetti *et al.*[6]

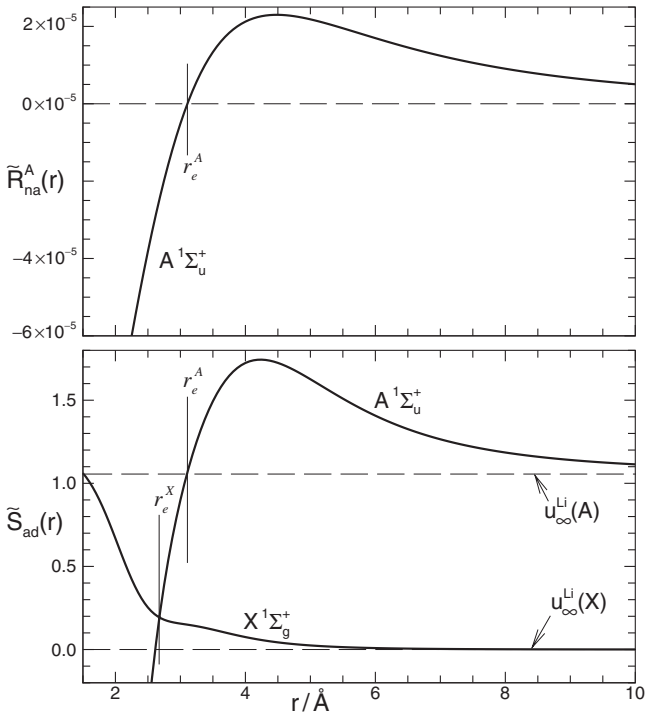

FIG. 5. BOB radial strength functions determined with $^{7,7}Li_2$ as the reference isotopologue: $\tilde{S}_{ad}(r)$ has units cm^{-1}, while $\tilde{R}_{ad}(r)$ is dimensionless.

2. BOB effects and isotopologue differences

Plots of the BOB radial strength functions determined in this analysis are shown in Fig. 5. The fact that $\tilde{S}_{ad}^X(\infty) - \tilde{S}_{ad}^X(r_e^X) = u_\infty - u_0 = -u_0$ is negative means that $\mathfrak{D}_e(X)$ is larger for $^{6,6}Li_2$ than for $^{7,7}Li_2$, while for the $A\ ^1\Sigma_u^+$ state $u_0 \approx u_\infty$, so the second term in Eq. (33) is dominant and the well depth for $^{6,6}Li_2$ is slightly smaller than that for $^{7,7}Li_2$. The first row of Table IV lists some key properties of the recommended potentials of Table III, while the next four rows present the isotopic changes in those quantities due to addition of the mass-weighted adiabatic BOB correction functions $\tilde{S}_{ad}(r)$ and the nonadiabatic correction term $\Delta V_{na}^A(r)$ of Eq. (31); the uncertainties in these shifts are defined by those of the fitted u_i values. The predicted value of $\mathfrak{D}_e^{tot}(A)$ for $^{6,7}Li_2$ shown in Table IV also incorporates the effect of the breakdown of g/u symmetry incorporated into its potential by Eq. (36).

The results of Table III were obtained from an analysis which treated $^{7,7}Li_2$ as the reference isotopologue. However, it is equally feasible to perform the global fit while defining $^{6,6}Li_2$ as the reference isotopologue. This would give us explicit MLR potentials for $^{6,6}Li_2$, rather than potentials obtained by adding the adiabatic difference potentials $\Delta V_{ad}^{(6,6)}(r)$ to potentials for $^{7,7}Li_2$. A fit performed in this way has *exactly* the same dimensionless rms deviation (to five decimal places) as does the fit with $^{7,7}Li_2$ as the reference isotopologue, and yields the results shown in the last row of Table IV; an alternate version of Table III obtained in this manner is included with the supplementary data submitted to the journal's online www archive.[48] The agreement between the results in the last two rows of this table attests to the validity of the effective adiabatic BOB radial strength functions determined herein.

TABLE IV. Some properties of the major isotopologues, with energies in cm^{-1} and lengths in angstrom, with shifted properties of the minor isotopologues calculated from Eqs. (28)–(35).

Fit	Isot.	$\mathfrak{D}_e(X)$	$\mathfrak{D}_e^{tot}(A)$	$T_e(A-X)$	$r_e(X)$	$r_e^{tot}(A)$	$C_3^\Sigma(A)$
3-isot	$^{7,7}Li_2$	8516.709(4)	9352.172(4)	14 068.185(12)	2.672 993(2)	3.107 950(5)	357 829.(8)
	change	0.032(2)	−0.081(2)	−0.062(2)	−0.000 003(2)	0.000 043(5)	8.(7)
	$^{6,7}Li_2$	8516.741(5)	[9351.915(5)][a]	14 068.123(12)	2.672 990(3)	3.107 993(6)	357 837.(11)
	change	0.065(3)	−0.162(3)	−0.124(4)	−0.000 005(4)	0.000 086(7)	15.(15)
	$^{6,6}Li_2$	8516.774(5)	9352.010(6)	14 068.061(13)	2.672 988(5)	3.108 036(9)	357 844.(17)
3-isot	$^{6,6}Li_2$	8516.774(4)	9352.010(4)	14 068.061(12)	2.672 986(2)	3.108 035(5)	357 845.(9)

[a]This value for $^{6,7}Li_2$ includes the shift by $-(1/2)\delta E_{^7Li}^{^6Li}(^2P_{1/2})$ introduced by g/u symmetry breakdown; see Sec. IV D.

3. Tests of the long-range potential coefficients

As indicated above and in Table III, our final results for this system were obtained with C_6, C_8, and C_{10} for the $X\ ^1\Sigma_g^+$ state and C_6^Σ and C_8^Σ for the $A\ ^1\Sigma_u^+$ state held fixed at values obtained from theory.[49,50] An examination of the effect of allowing some of these parameters either to vary in the fits or to be fixed at other values yielded the results summarized in Tables V and VI. For reference, the first row of each of these tables lists results for the recommended model of Table III.

The second row of Table V shows that when $C_6^\Sigma(A\ ^1\Sigma_u^+)$ was also treated as a free parameter, the overall quality of fit did not improve significantly, and the predicted uncertainty in the resulting C_6 value is almost as big as the difference between this fitted value and the current best theoretical value for this state.[49] We see no reason to prefer this fitted value to the theoretical value of Yan *et al.*,[49] which is believed to be accurate to better than 0.1%,[63] so the latter was used in the final recommended model of Table III. The third and fourth rows of this table provide additional evidence that the analysis is not very sensitive to the value of $C_6^\Sigma(A)$, since replacing the variational $C_6(A)$ value of Yan *et al.*[49] with the slightly less accurate (differing by 0.06%) value of Zhang *et al.*[50] or the earlier value of Marinescu and Dalgarno[64] (differing by 0.44%) had almost no effect on the quality of fit or the resulting well depth, and very little effect on the fitted C_3 coefficient.

For the A-state C_3^Σ value the situation is distinctly different. The fifth row of Table V shows that when this coefficient was also held fixed at the current best theoretical value,[49] the rms deviation from the 17 477 data increased by 1.0%. This large change indicates that the 0.020% difference between our fitted C_3^Σ coefficient and the current best theoretical value truly is significant. This high sensitivity of our analysis to the C_3^Σ coefficient is due to the fact that the experimental data extend well into the very long-range region where the slopes of the curves in Fig. 3 increase sharply due to the transition from case (a) to case (c) coupling, and the position and shape of this "bend" are sharply defined by that C_3^Σ value. A further demonstration of this sensitivity is provided by the fact that use of the C_3^Σ value of Zhang *et al.*,[50] which differs from our fitted value by only 0.051%, causes a massive 6.6% increase $\overline{dd}$ (last row of Table V). While the predicted uncertainty of only 0.0021% in our fitted C_3^Σ may be somewhat optimistic (see below), it seems clear that this analysis yields a distinctly more accurate value of $C_3^\Sigma(A\ ^1\Sigma_u^+)$, and hence also of the atomic $^2P_{1/2}\rightarrow{}^2S_{1/2}$ radiative lifetime, than does the best existing theoretical calculation.[49]

The situation for the $X\ ^1\Sigma_g^+$ state is again somewhat different. The middle row in Table VI shows that when the leading X-state long-range coefficient C_6 was treated as a free parameter in the fit, the quality of the fit improved by only 0.12% and the resulting C_6 value disagrees with the best available theoretical value[49] by only 2.2%. However, this difference is three times larger than the parameter uncertainty implied by the fit, and more than an order of magnitude larger than the uncertainty associated with that theoretical value. The last row of Table VI then shows that even larger uncertainties in the fitted C_6 arise if the second long-range coefficient (C_8) is also treated as a free parameter; in this case the differences are much smaller than the parameter uncertainties. In view of this pronounced model dependence of the fitted C_6 value, and the fact that the data region[23] only extends to 12.5 Å, we believe that these fitted values are less reliable than the theoretical values. This reinforces our decision to fix the three X-state dispersion coefficients at the values of Yan *et al.*[49] in the recommended model of Table III.

TABLE V. Effect on the fit of fixing vs floating the C_3 and C_6 coefficients for the $A\ ^1\Sigma_u^+$ state of Li_2.

$C_3^\Sigma/(cm^{-1}\ Å^3)$	$C_6^\Sigma/(10^7\ cm^{-1}\ Å^6)$	$\overline{dd}$	$\mathfrak{D}_e^{tot}/cm^{-1}$
357 829.2 (76)	[1.000 045][a]	1.005 88	9352.1725 (44)
357 856.9 (190)	0.952 (30)	1.005 75	9352.1723 (44)
357 828.8 (76)	[1.000 65][b]	1.005 89	9352.1725 (44)
357 831.7 (76)	[0.9957][c]	1.005 83	9352.1724 (44)
[357 758.0][a]	[1.000 045][a]	1.015 77	9352.1731 (45)
[358 011.0][b]	[1.000 65][b]	1.068 96	9352.1707 (47)

[a]From Yan *et al.* (Ref. 49).
[b]From Zhang *et al.* (Ref. 50).
[c]From Marinescu *et al.* (Ref. 64).

TABLE VI. Effect on the fit of fixing vs freeing the C_6 and C_8 coefficients for the $X\ ^1\Sigma_g^+$ state of Li_2.

$C_6/(10^6\ cm^{-1}\ Å^6)$	$C_8/(10^8\ cm^{-1}\ Å^8)$	$\overline{dd}$	$\mathfrak{D}_e/cm^{-1}$
[6.715 27][a]	[1.125 88][a]	1.005 88	8516.7091 (42)
6.862 (45)	[1.125 88][a]	1.004 69	8516.7166 (48)
6.803 (160)	1.25 (34)	1.004 67	8516.7160 (49)

[a]From Yan *et al.* (Ref. 49).

TABLE VII. Comparison of well depths (in cm^{-1}) and C_3^{Σ} coefficients (in cm^{-1} $Å^3$) determined herein with previously reported values.

	$X\ ^1\Sigma_g^+$		$A\ ^1\Sigma_u^+$			
	$\mathfrak{D}_e(^{7,7}Li_2)$	$\mathfrak{D}_e(^{6,6}Li_2)$	$\mathfrak{D}_e^{tot}(^{7,7}Li_2)$	$\mathfrak{D}_e^{tot}(^{6,6}Li_2)$	$10^5\times C_3^{\Sigma}(^{7,7}Li_2)$	$10^5\times C_3^{\Sigma}(^{6,6}Li_2)$
Barakat *et al.*[a] (1986)	8516.78(54)	⋯	⋯	⋯	⋯	⋯
Linton *et al.*[b] (1996)	⋯	8517.03(5)	⋯	9352.27(5)	⋯	3.58(1)
McAlexander *et al.*[c] (1996)	⋯	⋯	9352.10(18)	9352.18(8)	3.578 22(77)	3.578 52(73)
Martin *et al.*[d] (1997)	⋯	⋯	⋯	9352.032(12)	⋯	3.5749(15)
Coxon & Melville[e] (2006)	8516.769(8)	8516.74(1)	9352.06(8)	9351.96(1)	[3.584][f]	[3.584][f]
Present	8516.709(4)	8516.774(4)	9352.172(4)	9352.010(4)	3.578 29(9)	3.578 45(9)

[a]Reference 10.
[b]Reference 11.
[c]Reference 4.
[d]Reference 12.
[e]Reference 24.
[f]Reference 41.

4. Well depths and potentials: Then and now

Table VII compares the present results (last row) with the best previous empirical estimates of the well depths of the $X\ ^1\Sigma_g^+$ and $A\ ^1\Sigma_u^+$ states, and of the A-state C_3^{Σ} coefficient. The earliest estimate of the Li_2 dissociation energy with an uncertainty of less than $\sim 100\ cm^{-1}$ was obtained by Barakat *et al.*[10] from fluorescence transitions extending to the second-highest vibrational level of $^{7,7}Li_2$, $v(X)=40$, which (we now know) is bound by only $1.96\ cm^{-1}$. A decade later Linton *et al.*[11] reported a study of fluorescence into levels of the $A(^1\Sigma_u^+)$-state of $^{6,6}Li_2$ extending to $v(A)=84$, which is bound by only $2.72\ cm^{-1}$. However, their analysis assumed that the long-range potential was a simple sum of inverse-power terms, overlooking the transition from case (a) to case (c) behavior. As a result, their extrapolation is expected to approach a nonphysical limit corresponding to the weighted average of the $^6Li(^2P_{1/2})$ and $^6Li(^2P_{3/2})$ asymptotes (analogous to the dashed curve for $^{7,7}Li_2$ in Fig. 4). Hence, their A and X dissociation energies are expected to be $\approx 0.22\ cm^{-1}$ too large, as is seen to be the case. That same year McAlexander *et al.*[4] combined the PAS binding energies of Abraham *et al.*[1] with spectroscopic data for lower levels[11,13] to obtain estimates of the A-state well depth for both homonuclear isotopologues. However, since their analysis treated the long-range potential of the A state as a simple sum of inverse-power terms, their dissociation energies are less accurate than those obtained here or in Ref. 12. In contrast, using essentially the same $^{6,6}Li_2$ data, Martin *et al.*[12] obtained a distinctly better dissociation energy by basing their long-range potential on the Aubert-Frécon expression of Eq. (9).

In all studies prior to 2006 the potential energy functions were represented as arrays of RKR turning points attached to analytic long-range functions for extrapolating to the asymptote. In addition to error due to the first-order semiclassical nature of the RKR procedure, uncertainties regarding how the long-range tail should best be attached, and the problem of correcting for irregularities in inner-wall behavior, this approach always has uncertainties associated with the choices of the density of calculated RKR points and the interpolation procedure used for calculations on the resulting potential. It is also difficult to obtain a unified combined-isotopologue description in this way. In contrast, the DPF treatment of Coxon and Melville[24] yielded unified analytic potentials for all isotopologues in both states, which fully represented their data set to quantum mechanical accuracy. However, their analysis did not incorporate the PAS data for the A state and lacked access to the new data reported here. More seriously, the potential form they used could only take account of the single longest-range inverse-power contribution to the potential, and it did not attempt to take account of the A-state switchover from case (a) to case (c) behavior at very long range. As a result, their $A\ ^1\Sigma_u^+$ state potentials extrapolate to the nonphysical weighted average of the $Li(^2P_{1/2})$ and $Li(^2P_{3/2})$ asymptotes mentioned above (see the black dashed curve for $^{7,7}Li_2$ in Fig. 4). Since they were aware of this shortcoming, their recommended A-state dissociation energies (see Table VII) were obtained after subtracting a $0.224\ cm^{-1}$ shift from the fitted potential function well depths. However, this leaves us with a small inconsistency between their recommended dissociation energy and the well depth of their potential. In contrast, the analytic potentials obtained in the present work provide a unified description of all of the experimental data while incorporating sophisticated multiterm long-range potentials and the effect of spin-orbit interactions near the A-state asymptote within their form. However, it is important to remember that our A-state potential is defined as the generalized MLR potential of Table III *plus* the nonadiabatic BOB term of Eq. (31), so the MLR parameters $\mathfrak{D}_e$ and r_e for that state listed in Table III do not themselves represent the overall well depth $\mathfrak{D}_e^{tot}$ and equilibrium distance r_e^{tot} of that state.

5. The radiative lifetime of Li(2p) and its isotope dependence

The results in Table IV indicate that the values we obtain for C_3^{Σ} with $^{7,7}Li_2$ versus $^{6,6}Li_2$ as the reference isotopologue (last column of rows one and six) have marginally overlapping uncertainties, and both are $\sim 0.02\%$ larger than the theoretical value of Yan *et al.*[49] However, the latter is a variational "clamped-nuclei" value, which is implicitly based on the assumption of infinite nuclear masses, and hence is not expected to be precisely comparable to our empirical "real molecule" values. Theory suggests that long-range potential coefficients should have a weak dependence on the inverse of the molecular reduced mass;[35,59,65] hence, Fig. 6 plots our values as open round points joined by a line connecting them to the Yan *et al.* value placed at $\mu^{-1}=0$. We note too that the 0.024% difference between our fitted values of C_3^{Σ} and the

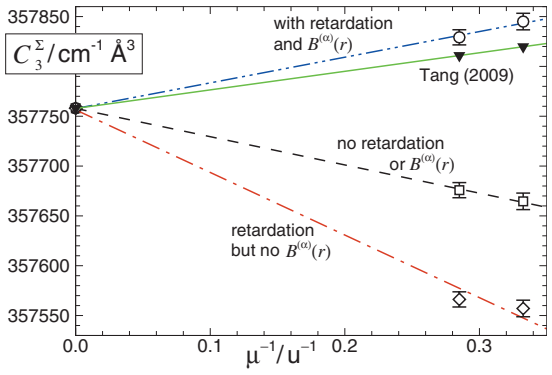

FIG. 6. Open points: isotopologue dependence of empirical C_3^{Σ} coefficients determined with three versions of the model Hamiltonian; the broken lines join the points for a given model to the "mass-infinity" theoretical value of Yan *et al.* (Ref. 49). Solid triangular points joined by a solid line are the very recent theoretical values of Tang *et al.* (Ref. 74).

variational value of Yan *et al.*[49] is very close to the 0.018% difference predicted by an expression for the isotopologue dependence of long-range C_n coefficients reported by de Lange *et al.*[59] The systematic behavior of this plot strongly suggests that notwithstanding the overlapping uncertainties, the difference between our C_3^{Σ} values for $^{6,6}Li_2$ and $^{7,7}Li_2$ is physically significant.

The open square and open diamond-shaped points on Fig. 6 show how our fitted C_3^{Σ} values are affected if one or both of the retardation correction or the nonadiabatic $2B^{(\alpha)}(r)$ correction of Eq. (31) had been omitted from the model. As was found by McAlexander *et al.*,[4] the effect of including the $B^{(\alpha)}(r)$ term is much larger (here, by a factor of $\sim$2.7) and of opposite sign to the effect of including retardation in the model.

The parameter uncertainties shown in Tables III–V are simply the correlated 95% confidence limit uncertainties associated with the fit to a particular model, and they do not take account of model dependence–the sensitivity of the fitted parameter to details of the model used in the analysis. To obtain some estimate of the effect of model dependence on our C_3^{Σ} values, the global least-squares fit was repeated for a range of models which were similar to those of Table III, but which used different exponent polynomial orders (15, 16, or 17), different $r_{\rm ref}^A$ values (ranging from 3.5 to 5.5) and different $q_{\rm ad}$ values. Averaging over results for 26 of these cases for which the quality-of-fit $\overline{dd}$ values lay within 1% of that for the best fit yields $C_3^{\Sigma}(^{7,7}Li_2)=357\,835(\pm 13)$ cm^{-1} Å^3. While no finite test of model dependence can be exhaustive, we take this to indicate that a more realistic overall uncertainty in our fitted C_3^{Σ} value would be double that given in Table III to $\pm 0.005\%$. Thus, our final estimates of the values of C_3^{Σ} for $^{7,7}Li_2$ and $^{6,6}Li_2$ are $357\,829.(\pm 18.)$ and $357\,845.(\pm 18.)$ cm^{-1} Å^3.

The resonant dipole-dipole long-range potential coefficient C_3^{Σ} for the $A\ ^1\Sigma_u^+$ state of Li_2 is related to the radiative lifetime of Li($2p$) atoms by the expression[4]

$$\tau(2p)=\frac{3}{4\pi c}\frac{(\lambda_{SP}/2\pi)^3}{C_3^{\Sigma}}, \tag{37}$$

in which the speed of light c has units (cm/s), the $^2P-^2S$ transition wavelength λ_{SP} has units (Å), and the units of C_3^{Σ} are [cm^{-1} Å^3]. Applying this expression to our fitted C_3^{Σ} values yields $\tau(2p)=27.1018(\pm 0.0014)$ ns for ^{7}Li and $27.1024(\pm 0.0014)$ ns for ^{6}Li. Within the uncertainties, these results are in almost exact agreement with the best previous value reported for this system, $27.102(\pm 0.007)$ ns,[4] but the uncertainties in the present values are a factor of 5 smaller.

V. DISCUSSION AND CONCLUSIONS

A combined analysis of the 17 477 available data for the $A-X$ and $E,F-A$ systems of $^{7,7}Li_2$, $^{6,6}Li_2$, and $^{6,7}Li_2$ yielded analytic potential energy functions for the $X\ ^1\Sigma_g^+$ and $A\ ^1\Sigma_u^+$ states which (on average) explain all of those data within the experimental uncertainties ($\overline{dd}=1.0059$). The radial ranges spanned by the vibrational turning points of levels involved in this analysis are 1.8–12.5 Å for the X state and 2.0–89.8 Å for the A state. This analysis yields improved dissociation energies of $\mathfrak{D}_e(X)=8516.709(\pm 0.004)$ and $\mathfrak{D}_e^{\rm tot}(A)=9352.172(\pm 0.004)$ cm^{-1} for $^{7,7}Li_2$, of $\mathfrak{D}_e(X)=8516.774(\pm 0.004)$ and $\mathfrak{D}_e^{\rm tot}(A)=9352.010(\pm 0.004)$ cm^{-1} for $^{6,6}Li_2$, and of $\mathfrak{D}_e(X)=8516.741(\pm 0.005)$ and $\mathfrak{D}_e^{\rm tot}(A)=9351.915(\pm 0.005)$ cm^{-1} for $^{6,7}Li_2$. Note that this $\mathfrak{D}_e^{\rm tot}$ value for the A-state of $^{6,7}Li_2$ includes the adjustment $-(1/2)\delta E_{^7{\rm Li}}^{^6{\rm Li}}(^2P_{1/2})$ associated with g/u symmetry breakdown, as discussed in Sec. IV C.

Lists of band constants $\{G_v,B_v,D_v,\cdots,$ etc.$\}$ for all bound vibrational levels of the $X\ ^1\Sigma_g^+$ state of all three Li_2 isotopologues, as well as for all bound levels of the $A\ ^1\Sigma_u^+$ state of $^{6,7}Li_2$, were generated from the present recommended potentials and included in the data submitted to the journal's online www archive.[48] Using the new integration technique of Ref. 66, analogous band constants were also generated for all vibrational levels of the $A\ ^1\Sigma_u^+$ states of $^{7,7}Li_2$ and $^{6,6}Li_2$ bound by more than 0.000 05 cm^{-1}, including ten levels of each species with binding energies of less than 0.1 cm^{-1}. While this approach should be able to determine *all* vibrational levels of this state, no matter how weakly bound,[66] our current computer codes only use double-precision (REAL*8) arithmetic, and the somewhat complicated form of the function $u_{\rm LR}^{A,{\rm tot}}(r)$ defining the long-range tail of our analytic potential means that higher precision would be required to obtain stable results for levels even closer to the limit. However, this has little practical importance, since it is clear that if the effect of retardation must be considered for the resonance dipole-dipole interaction, it should also be incorporated into the dispersion terms and the long-range tail of the adiabatic correction represented by Eq. (31), and our overlooking that behavior would prevent us from making reliable predictions for levels extremely close to the limit. This problem does not arise for $^{6,7}Li_2(A\ ^1\Sigma_u^+)$ because g/u symmetry breakdown means that its potential function asymptotically dies off as $1/r^6$ rather than $1/r^3$, and the lower density of states near its asymptote mean that the precision problem mentioned above does not arise. At the same time, the somewhat *ad hoc* nature of our g/u breakdown correction for this species means the predicted binding energies of level above $v(A)=83$ will have uncertainties of 0.5% or larger. Note too that the results described above neglect the effects of hyperfine coupling, which becomes

non-negligible very near the potential asymptotes. However, the potential functions obtained herein should provide an optimum zeroth order description as a basis for efforts to account for such effects.

One disappointment of the present analysis is the fact that our model cannot represent the observed PAS datum for $v(A)=83$ of $^{6,7}Li_2$ within the reported experimental uncertainty of 0.0007 cm^{-1}, our calculated binding energy for this level being 0.0086 cm^{-1} larger than the experimental value. This discrepancy is in the wrong direction to expect it to be accounted for by a proper four-state treatment of the effect of g/u symmetry breakdown, and it remains a puzzle. To prevent this outlier datum from having an undue effect on the results, the reported uncertainty[25] was replaced by 0.007 cm^{-1} in our final fits.

The present work also yields resonance-dipole interaction coefficients $C_3^{\Sigma}=357\,829.(\pm 18)$ and $357\,845(\pm 18)$ cm^{-1} Å^3 for the $A\,^1\Sigma_u^+$ states of $^{7,7}Li_2$ and $^{6,6}Li_2$, respectively. They in turn yield $^2P-^2S$ radiative lifetimes with significantly smaller uncertainties that the best previous estimates for this system. Indeed, our radiative lifetimes have smaller percent uncertainties (typically, by more than an order of magnitude) than those obtained from analyses of PAS data for any of Na, K, Rb, Cs, Ca, Sr, and Yb.[55,67–73] The 0.02% difference between these experimental C_3^{Σ} coefficients [and the $\tau(2p)$ value] and the theoretical value of Yan *et al.*[49] is probably due neglect the effect of the finite magnitudes of the nuclear masses in those 1996 calculations.

Calculations using our potentials for the $X\,^1\Sigma_g^+$ states of $^{7,7}Li_2$ and $^{6,6}Li_2$ yield predicted scattering lengths for these species of $18.11(\pm 0.05)$ and $23.84(\pm 0.05)$ Å, respectively. The uncertainties in these quantities were estimated from the model dependence of predictions generated using potentials with slightly different parametrization (i.e., different exponent polynomial orders or different values of $r_{\rm ref}$) which were obtained from fits of equivalent quality.

An essential feature of the present analysis has been the explicit inclusion in the analytic MLR potential of an expression for the long-range potential of the $A\,^1\Sigma_u^+$ state which incorporates the transition between case (a) and case (c) coupling at large internuclear distances. This is a very telling illustration of the utility and capabilities of this potential function form. This work also introduced two other generalizations of the MLR form which allow one to obtain much more compact and robust fitted potential energy functions than would otherwise be possible.

Finally, we note that after the above work was complete, Tang *et al.*[74] reported very accurate new variational calculations for atomic Li which did take account of finite nuclear mass effects and yielded new isotopologue-dependent dispersion and resonance-dipole C_n coefficients for a number of electronic states. For the $X\,^1\Sigma_g^+$ state of $^{7,7}Li_2$ the new C_6, C_8, and C_{10} values are 0.047%, 0.036%, and 0.028% larger than those used in the present study, while for the $A\,^1\Sigma_u^+$ state the new C_6 and C_8 values are, respectively, 0.0050% larger and 0.067% smaller than those used here. Repeating the fit to our final model with these coefficients fixed at the new values of Tang *et al.* essentially had no effect on the quality of fit or on the resulting values of the physically interesting parameters $\mathfrak{D}_e$, r_e, or C_3^{Σ}. These new theoretical C_3^{Σ} values for the $A\,^1\Sigma_u^+$ state of $^{7,7}Li_2$ and $^{6,6}Li_2$ and "mass-infinity" Li_2 are shown as solid triangular points joined by a solid line in Fig. 6. When our final fit was repeated with C_3^{Σ} for $^{7,7}Li_2$ also fixed at the new theoretical value, the quality of fit became slightly worse, $\overline{dd}=1.006\,47$ versus $1.005\,88$, although the associated changes in $\mathfrak{D}_e$ and r_e are less than 1 unit in the last digit quoted in Table III. Overall, we prefer our experimental values of C_3^{Σ}, and attribute the remaining 0.005% difference with theory to relativistic and quantum electrodynamics effects which were not considered in the calculations of Ref. 74.

ACKNOWLEDGMENTS

We are grateful to Dr. Donald K. Hsu for providing us with a hard copy listing of the very extensive set of high quality $A-X$ data for $^{7,7}Li_2$ obtained as part of his Ph.D. thesis research, and to Professors Jim Mitroy of Charles Darwin University and Zong-Chao Yan of the University of New Brunswick for helpful discussions regarding the reliability of the theoretical long-range coefficients. This research was supported by the Natural Science and Engineering Research Council of Canada (NSERC) through the award of Discovery Grants to R.J.L. and C.L., and a USRA fellowship to N.D.

[1] E. R. I. Abraham, N. W. M. Ritchie, W. I. McAlexander, and R. G. Hulet, J. Chem. Phys. **103**, 7773 (1995).
[2] C. C. Bradley, C. A. Sackett, and R. G. Hulet, Phys. Rev. Lett. **78**, 985 (1997).
[3] W. I. McAlexander, E. R. I. Abraham, N. W. M. Ritchie, C. J. Williams, H. T. C. Stoof, and R. G. Hulet, Phys. Rev. A **51**, R871 (1995).
[4] W. I. McAlexander, E. R. I. Abraham, and R. G. Hulet, Phys. Rev. A **54**, R5 (1996).
[5] J. Weiner, V. S. Bagnato, S. Zilio, and P. S. Julienne, Rev. Mod. Phys. **71**, 1 (1999).
[6] C. J. Sansonetti, B. Richou, R. Engleman, Jr., and L. J. Radziemski, Phys. Rev. A **52**, 2682 (1995).
[7] P. Qi, J. Bai, E. Ahmed, A. Lyyra, S. Kotochigova, A. Ross, C. Effantin, P. Zalicki, J. Vigué, G. Chawla, R. Field, T.-J. Whang, W. Stwalley, H. Knöckel, E. Tiemann, J. Shang, L. Li, and T. Bergeman, J. Chem. Phys. **127**, 044301 (2007).
[8] O. Docenko, M. Tamanis, R. Ferber, E. Pazyuk, A. Zaitsevskii, A. Stolyarov, A. Pashov, H. Knöckel, and E. Tiemann, Phys. Rev. A **75**, 042503 (2007); **75**, 059905(E) (2007).
[9] D. K. Hsu, "The absorption spectra of the $A-X$ and $C-X$ transitions of the ($^7Li_2$) lithium molecule," Ph.D. dissertation, Fordham University, 1975.
[10] B. Barakat, R. Bacis, F. Carrot, S. Churassy, P. Crozet, F. Martin, and J. Vergès, Chem. Phys. **102**, 215 (1986).
[11] C. Linton, F. Martin, I. Russier, A. J. Ross, P. Crozet, S. Churassy, and R. Bacis, J. Mol. Spectrosc. **175**, 340 (1996).
[12] F. Martin, M. Aubert-Frécon, R. Bacis, P. Crozet, C. Linton, S. Magnier, A. Ross, and I. Russier, Phys. Rev. A **55**, 3458 (1997).
[13] K. Urbanski, S. Antonova, A. Yiannopoulou, A. M. Lyyra, L. Li, and W. C. Stwalley, J. Chem. Phys. **104**, 2813 (1996); **116**, 10577(E) (2002).
[14] X. Wang, J. Yang, J. Qi, and A. M. Lyyra, J. Mol. Spectrosc. **191**, 295 (1998).
[15] X. Wang, J. Magnes, A. M. Lyyra, A. J. Ross, F. Martin, P. M. Dove, and R. J. Le Roy, J. Chem. Phys. **117**, 9339 (2002).
[16] A. Adohi-Krou, F. Martin, A. J. Ross, C. Linton, and R. J. Le Roy, J. Chem. Phys. **121**, 6309 (2004).
[17] R. Rydberg, Z. Phys. **73**, 376 (1931); O. Klein, *ibid.* **76**, 226 (1932); R. Rydberg, *ibid.* **80**, 514 (1933); A. L. G. Rees, Proc. Phys. Soc. London **59**, 998 (1947).

[18] R. N. Zare, University of California Lawrence Radiation Laboratory Report No. UCRL-10925, 1963.
[19] R. N. Zare, J. Chem. Phys. **40**, 1934 (1964).
[20] R. J. Le Roy, "RKR1 2.0: A computer program implementing the first-order RKR method for determining diatomic molecule potential energy curves," University of Waterloo Chemical Physics Research Report No. CP-657, 2003, see http://leroy.uwaterloo.ca/programs/.
[21] W. M. Kosman and J. Hinze, J. Mol. Spectrosc. **56**, 93 (1975).
[22] C. R. Vidal and H. Scheingraber, J. Mol. Spectrosc. **65**, 46 (1977).
[23] The data region is defined here as the distance between the outer and inner turning points of the highest-energy vibrational level for which data are available.
[24] J. A. Coxon and T. C. Melville, J. Mol. Spectrosc. **235**, 235 (2006).
[25] U. Schlöder, C. Silber, T. Deuschle, and C. Zimmermann, Phys. Rev. A **66**, 061403 (2002).
[26] S. Antonova, G. Lazarov, K. Urbanski, A. Lyyra, L. Li, G.-H. Jeung, and W. Stwalley, J. Chem. Phys. **112**, 7080 (2000).
[27] R. J. Le Roy, Y. Huang, and C. Jary, J. Chem. Phys. **125**, 164310 (2006).
[28] R. J. Le Roy and R. D. E. Henderson, Mol. Phys. **105**, 663 (2007).
[29] H. Salami, A. J. Ross, P. Crozet, W. Jastrzebski, P. Kowalczyk, and R. J. Le Roy, J. Chem. Phys. **126**, 194313 (2007).
[30] A. Shayesteh, R. D. E. Henderson, R. J. Le Roy, and P. F. Bernath, J. Phys. Chem. A **111**, 12495 (2007).
[31] Y. Huang and R. J. Le Roy, J. Chem. Phys. **119**, 7398 (2003); **126**, 169904(E) (2007).
[32] H. Margenau, Rev. Mod. Phys. **11**, 1 (1939).
[33] J. O. Hirschfelder, C. F. Curtiss, and R. B. Bird, *Molecular Theory of Gases and Liquids* (Wiley, New York, 1964).
[34] T. Y. Chang, Rev. Mod. Phys. **39**, 911 (1967).
[35] J. O. Hirschfelder and W. J. Meath, in *Intermolecular Forces*, Adv. Chem. Phys. Vol. 12, edited by J. O. Hirschfelder (Interscience, New York, 1967), Chap. 1, pp. 3–106.
[36] W. J. Meath, Am. J. Phys. **40**, 21 (1972).
[37] R. J. Le Roy and R. B. Bernstein, J. Chem. Phys. **52**, 3869 (1970).
[38] R. J. Le Roy, in *Molecular Spectroscopy*, edited by R. N. Barrow, D. A. Long, and D. J. Millen (Chemical Society of London, London, 1973), Vol. 1, Specialist Periodical Report 3, pp. 113–176.
[39] This "usual" case assumes that one or both of the ion and neutral particles formed when the state dissociates is in an S electronic state. If this is not true, the long-range potential for such states will also include a C_5/r^5 term.
[40] M. Movre and G. Pichler, J. Phys B **10**, 2631 (1977).
[41] B. Bussery and M. Aubert-Frécon, J. Chem. Phys. **82**, 3224 (1985).
[42] M. Aubert-Frécon, G. Hadinger, S. Magnier, and S. Rousseau, J. Mol. Spectrosc. **188**, 182 (1998).
[43] R. McLone and E. Power, Mathematika **11**, 91 (1964).
[44] W. J. Meath, J. Chem. Phys. **48**, 227 (1968).
[45] R. J. Le Roy and Y. Huang, J. Mol. Struct.: THEOCHEM **591**, 175 (2002).
[46] R. J. Le Roy, D. R. T. Appadoo, K. Anderson, A. Shayesteh, I. E. Gordon, and P. F. Bernath, J. Chem. Phys. **123**, 204304 (2005).
[47] R. J. Le Roy, J. Tao, C. Haugen, R. D. E. Henderson and Y.-R. Wu (unpublished).
[48] See EPAPS supplementary material at 10.1063/1.3264688 for ASCII files containing listings of the data used in the present work, for tabulations of the vibrational energies and rotational constants of the $X\ ^1\Sigma_u^+$ and $A\ ^1\Sigma_u^+$ states for all three isotopologues of Li_2 generated from our final recommended potentials, and for a set of potential function parameters equivalent to those in Table III, but obtained from a fit which treated $^{6,6}Li_2$ as the reference isotopologue.
[49] Z.-C. Yan, J. F. Babb, A. Dalgarno, and G. W. F. Drake, Phys. Rev. A **54**, 2824 (1996).
[50] J.-Y. Zhang, J. Mitroy, and M. W. J. Bromley, Phys. Rev. A **75**, 042509 (2007).
[51] Analogous models combining $p=4$ with $q=2$ yielded equally good fits for $N_S=N_L=13$. However, $y_2(r)$ is too "soft" an expansion variable to yield reliable extrapolations, and the resulting potentials tended both to have nonphysical inflection points in the small-r extrapolation region and implausible fluctuations outside the "data region" at large r.
[52] J. K. G. Watson, J. Mol. Spectrosc. **80**, 411 (1980).
[53] J. K. G. Watson, J. Mol. Spectrosc. **223**, 39 (2004).
[54] R. J. Le Roy, J. Mol. Spectrosc. **194**, 189 (1999).
[55] F. Vogt, C. Grain, T. Nazarova, U. Sterr, F. Riehle, C. Lisdat, and E. Tiemann, Eur. Phys. J. D **44**, 73 (2007).
[56] The contribution to this isotope shift from the slope of $\widetilde{S}_{ad}(r)$ may be neglected, since it scales as the factor $[\widetilde{S}'_{ad}(r_e)]^2/(2\widetilde{k})$ which is $\sim 10^{-4}$ times smaller than u_0 or u_∞.
[57] The centrifugal BOB function $q^{(\alpha)}(r)$ makes no contribution to isotopic differences in r_e because of our adoption of Watson's convention (Refs. 52 and 53) that $q^{(\alpha)}(r_e)=0$ (i.e., that $t_0^{A/B}=0$).
[58] A. de Lange, E. Reinhold, W. Hogervorst, and W. Ubachs, Can. J. Phys. **78**, 567 (2000).
[59] A. de Lange, E. Reinhold, and W. Ubachs, Int. Rev. Phys. Chem. **21**, 257 (2002).
[60] R. J. Le Roy, J. Seto, and Y. Huang, "DPotFit 1.2: A computer program for fitting diatomic molecule spectra to potential energy functions," University of Waterloo Chemical Physics Research Report No. CP-664, 2007, see http://leroy.uwaterloo.ca/programs/.
[61] R. J. Le Roy, "betaFIT 2.0: A computer program to fit potential function points to selected analytic functions," University of Waterloo Chemical Physics Research Report No. CP-665, 2009, see http://leroy.uwaterloo.ca/programs/.
[62] R. J. Le Roy, J. Mol. Spectrosc. **191**, 223 (1998).
[63] J. Mitroy (private communication), 2009.
[64] M. Marinescu and A. Dalgarno, Phys. Rev. A **52**, 311 (1995).
[65] R. T. Pack and J. O. Hirschfelder, J. Chem. Phys. **52**, 521 (1970).
[66] V. V. Meshkov, A. V. Stolyarov, and R. J. Le Roy, Phys. Rev. A **78**, 052510 (2008).
[67] K. M. Jones, P. Julienne, P. D. Lett, W. D. Phillips, E. Tiesinga, and C. J. Williams, Europhys. Lett. **35**, 85 (1996).
[68] H. Wang, J. Li, X. Wang, C. Williams, P. Gould, and W. Stwalley, Phys. Rev. A **55**, R1569 (1997).
[69] R. Gutterres, C. Amiot, A. Fioretti, C. Gabbanini, M. Mazzoni, and O. Dulieu, Phys. Rev. A **66**, 024502 (2002).
[70] Y. Takasu, K. Komori, K. Honda, M. Kumakura, T. Yabuzaki, and Y. Takahashi, Phys. Rev. Lett. **93**, 123202 (2004).
[71] M. Yasuda, T. Kishimoto, M. Takamoto, and H. Katori, Phys. Rev. A **73**, 011403(R) (2006).
[72] N. Bouloufa, A. Crubellier, and O. Dulieu, Phys. Rev. A **75**, 052501 (2007).
[73] N. Bouloufa, A. Crubellier, and O. Dulieu, Phys. Scr. T **t134**, 014014 (2009).
[74] L.-Y. Tang, Z.-C. Yan, T.-Y. Shi, and J. F. Babb, Phys. Rev. A **79**, 062712 (2009).